Cell PRESS
Neuron
Article

Subunit Composition of Synaptic AMPA Receptors Revealed by a Single-Cell Genetic Approach

Wei Lu,[1] Yun Shi,[1] Alexander C. Jackson,[1] Kirsten Bjorgan,[1] Matthew J. During,[2] Rolf Sprengel,[3] Peter H. Seeburg,[3] and Roger A. Nicoll[1,*]
[1]Department of Cellular and Molecular Pharmacology, University of California, San Francisco, San Francisco, CA 94143, USA
[2]Department of Molecular Virology, Immunology, and Medical Genetics, Ohio State University, Columbus, OH 43210, USA
[3]Department of Molecular Neurobiology, Max Planck Institute for Medical Research, D-69120 Heidelberg, Germany
*Correspondence: nicoll@cmp.ucsf.edu
DOI 10.1016/j.neuron.2009.02.027

SUMMARY

The precise subunit composition of synaptic ionotropic receptors in the brain is poorly understood. This information is of particular importance with regard to AMPA-type glutamate receptors, the multimeric complexes assembled from GluA1-A4 subunits, as the trafficking of these receptors into and out of synapses is proposed to depend upon the subunit composition of the receptor. We report a molecular quantification of synaptic AMPA receptors (AMPARs) by employing a single-cell genetic approach coupled with electrophysiology in hippocampal CA1 pyramidal neurons. In contrast to prevailing views, we find that GluA1A2 heteromers are the dominant AMPARs at CA1 cell synapses (~80%). In cells lacking GluA1, -A2, and -A3, synapses are devoid of AMPARs, yet synaptic NMDA receptors (NMDARs) and dendritic morphology remain unchanged. These data demonstrate a functional dissociation of AMPARs from trafficking of NMDARs and neuronal morphogenesis. This study provides a functional quantification of the subunit composition of AMPARs in the CNS and suggests novel roles for AMPAR subunits in receptor trafficking.

INTRODUCTION

The advent of molecular biology and receptor cloning has resulted in extraordinary advances in our understanding of neurotransmitter receptors. Virtually all ionotropic receptors are multimeric structures composed of variable combinations of subunits. The function and trafficking of these receptors are critically dependent on their subunit composition. Based on the biophysical properties of heterologously expressed receptors; the expression pattern of the subunits; conventional gene knockout (KO) approaches; and, in rare instances, the discovery of subunit selective antagonists, the subunit composition of native synaptic receptors has been inferred but not unambiguously established.

We have focused on determining the subunit composition of AMPA-type ionotropic glutamate receptors (AMPARs) at the excitatory Schaffer collateral/commissural synapses onto CA1 hippocampal pyramidal cells, arguably the most-studied synapse in the brain. This synapse releases glutamate that acts on two types of ionotropic glutamate receptors, AMPARs and NMDARs. AMPARs are primarily responsible for the fast moment-to-moment communication at excitatory synapses and undergo rapid activity-dependent recruitment during synaptic plasticity. Four subunits, GluA1–A4 (GluR1–4 or GluR-A to -D) (Collingridge et al., 2008), contribute to the formation of heterotetrameric receptors (Dingledine et al., 1999; Hollmann and Heinemann, 1994; Mayer and Armstrong, 2004; Seeburg, 1993). The subunit composition of AMPARs has received a great deal of attention, as it has been proposed to dictate the mode of AMPAR trafficking (Bredt and Nicoll, 2003; Malinow and Malenka, 2002; Shepherd and Huganir, 2007). In addition, the biophysical properties of AMPARs are thought to depend on subunit composition (Cull-Candy et al., 2006; Isaac et al., 2007; Jonas, 2000). Thus the molecular quantification of synaptic AMPAR subunit composition has become paramount in understanding the mechanisms underlying AMPAR trafficking and synaptic plasticity. Yet, despite intensive research using a variety of approaches (Baude et al., 1995; Cheng et al., 2006; Geiger et al., 1995; Jensen et al., 2003; Sans et al., 2003; Shi et al., 2001; Wenthold et al., 1996), the precise subunit composition has remained elusive, even at the best-studied synapse in the brain.

We have used a single-cell genetic approach that combines the use of electrophysiology and conditional KO mice for GluA1, GluA2, and GluA3 (*GRIA1*$^{fl/fl}$, *GRIA2*$^{fl/fl}$, *GRIA3*$^{fl/fl}$) to delete each of the GluA subunits, either alone or in combination, by expressing Cre recombinase in individual CA1 hippocampal pyramidal cells. The subunit composition of synaptic and extrasynaptic AMPARs was determined by simultaneous whole-cell recording from Cre-expressing cells and neighboring control cells, as well as recording from somatic outside-out patches (OOPs). Comparing the results of single subunit deletions with multiple subunit deletions provided a cross-validation that was remarkably consistent, thus permitting a rigorous quantification of the subunit composition of AMPARs. We found that approximately 80% of synaptic and >95% of somatic extrasynaptic receptors are GluA1A2 heteromers. The remaining receptors are GluA2A3 heteromers. Importantly, the number and composition of synaptic NMDARs remain unchanged in the complete absence of AMPARs, and no obvious change in dendritic morphology was observed. The present results provide a

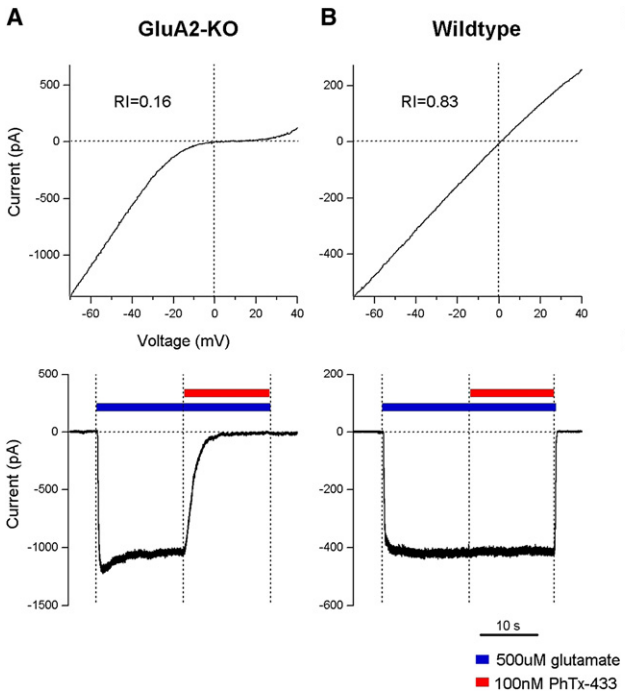

Figure 1. Outside-Out Patch Recordings of AMPAR-Mediated Current from CA1 Pyramidal Neurons in GluA2 KO and WT Mice

(A) (Top) Example of the strongly inwardly rectifying I/V curve of glutamate-evoked AMPAR-mediated current, in the presence of 100 μM cyclothiazide, from acute hippocampal slice from the germline 2- to 3-week-old GluA2-KO mouse, with an RI value of 0.16. (Bottom) In a subsequent glutamate application in the same OOP, held at −60 mV, ~99% of the current could be blocked by 100 nM PhTx-433.

(B) Example of the linear I/V curve of glutamate-evoked current in a WT littermate, with an RI value of 0.83. (Bottom) In the same OOP, glutamate-evoked current was untouched by 100 nM PhTx-433.

(C) Bar graph showing average RI values for each of the genotypes: GluA2-KO mice, RI = 0.12 ± 0.02 (n = 9); WT mice, RI = 0.82 ± 0.02 (n = 15).

(D) Bar graph showing the average percent block (%) of glutamate-evoked currents by 100 nM PhTx-433 in GluA2-KO mice; average percent block is 97.9% ± 0.4% (n = 6) and, in WT mice, 0% (n = 5).

quantification of the subunit composition of neurotransmitter receptors at synapses in the CNS, and facilitate understanding of AMPAR trafficking and synaptic plasticity in vivo. Furthermore, the approach outlined in this study of simultaneously deleting multiple genes in single cells is equally powerful in defining the specific roles of any family of related proteins.

RESULTS

All Surface AMPARs Contain GluA2 at CA1 Pyramidal Neurons

Of all the AMPAR subunits, GluA2 has the most impact on the biophysical properties of the resulting heteromeric complexes. AMPARs lacking the GluA2 subunit are strongly inwardly rectifying in the presence of intracellular polyamines and are Ca^{2+} permeable, whereas those that contain the GluA2 subunit have a linear or near-linear current-voltage (I/V) relationship and are impermeable to divalent cations (Cull-Candy et al., 2006; Isaac et al., 2007; Jonas, 2000). This unique property, conferred by the presence of the GluA2 subunit, is due to the Arg607 residue introduced into the GluA2 pore loop by RNA editing at the Q/R site (Sommer et al., 1991). Such properties are easily observed during electrophysiological recordings, the technique that we use throughout this paper to isolate the properties of fully functional, surface-expressed heteromeric AMPAR complexes.

There is general agreement that, under basal conditions, synaptic AMPARs at CA1 pyramidal neurons are composed of heteromeric receptors containing the edited GluA2 subunit (Bredt and Nicoll, 2003; Malinow and Malenka, 2002; Shepherd and Huganir, 2007). On the other hand, it is unclear whether extrasynaptic receptors, which abound on the surface of CA1 pyramidal cells and are proposed to serve as a reserve receptor pool for the synapse, have the same composition as synaptic receptors with respect to their GluA2 subunit content. This is an important issue, because biochemical studies have detected a small but significant population of GluA1 homomeric receptors in the hippocampus (Sans et al., 2003; Wenthold et al., 1996), and understanding the identity of extrasynaptic AMPARs is crucial for studying LTP.

Two standard methods were used to determine whether surface AMPARs in WT mice contain or lack the GluA2 subunit. The first method was to measure the I/V relationship of glutamate-evoked AMPAR currents in OOPs pulled from the soma of CA1 pyramidal neurons in acute slices. The second method involved determining the sensitivity of the AMPAR response to the polyamine toxin, philanthotoxin 433 (PhTx-433). GluA2-lacking receptors are strongly and selectively blocked by PhTx-433, whereas GluA2-containing receptors are not (Washburn and Dingledine, 1996).

Since the soma of CA1 pyramidal cells lack excitatory synapses (Megias et al., 2001), we used somatic OOPs to study the properties of extrasynaptic AMPARs. First we examined the properties of AMPAR responses in the germline GluA2 KO mouse that lacks GluA2 in every cell (Jia et al., 1996). We applied glutamate with cyclothiazide to these patches in the presence of APV, picrotoxin, and TTX as a way of isolating glutamate-evoked, AMPAR-mediated current. As expected, the I/V showed strong inward rectification (Figures 1A and 1C). A dose-response analysis demonstrated that the minimal concentration of PhTx-433 required to rapidly and completely block AMPAR-mediated currents in the GluA2 KO mouse was 100 nM (Figures 1A and 1D). We next examined the properties of extrasynaptic AMPARs in CA1 pyramidal neurons from wild-type (WT) mice. In this case, the I/V was near linear (Figures 1B and 1C), suggesting that all AMPARs contain GluA2. To confirm this, we found that glutamate-evoked current was untouched by the application of

100 nM PhTx-433 (Figures 1B and 1D). Our results, combined with previous work, indicate that GluA1 homomers—and indeed any AMPAR complex lacking GluA2—are excluded from the surface of CA1 pyramidal cells from animals at the age of 2–4 weeks under basal conditions.

Synapses Lacking GluA1, -A2, and -A3 Are Devoid of AMPARs but Are Otherwise Normal

Previously, germline AMPAR subunit deletions have been employed to study the contributions of individual subunits to synaptic transmission (Andrasfalvy et al., 2003; Jensen et al., 2003; Jia et al., 1996; Meng et al., 2003; Zamanillo et al., 1999). However, this traditional KO approach is potentially problematic for this specific question for at least two reasons. First, the absence of a protein throughout neurodevelopment could lead to compensatory changes that render the resulting cellular phenotype a false readout of the true contribution of the protein in the native condition (Elias et al., 2006). Second, in addition to the direct (desired) effect, germline deletion of an AMPAR allele has the potential to indirectly affect AMPARs by affecting the activity of presynaptic inputs and indeed the entire circuit behavior of the brain, producing undesired consequences on the activity-dependent development of excitatory synapses.

For these reasons, we used a different approach in an attempt to determine contributions of AMPAR subunits to synaptic transmission: we used conditional KO alleles for GluA1 (Engblom et al., 2008), GluA2 (Shimshek et al., 2005), and GluA3 (see the Experimental Procedures) and created homozygous gene-targeted mouse strains for each (*GRIA1*$^{fl/fl}$, *GRIA2*$^{fl/fl}$, and *GRIA3*$^{fl/fl}$). To eliminate the target gene, Cre recombinase was expressed in a small set of hippocampal neurons either by inoculating the hippocampus of P0–P2 mice by transcranial stereotactic injection with a recombinant adeno-associated virus expressing Cre covalently bound to GFP (rAAV-Cre-GFP) or biolistic transfection of a Cre-IRES-GFP construct in hippocampal slice cultures from P5–P7 mice. With both P0 injections and slice cultures, we could genetically alter a small percentage of hippocampal neurons, thus minimizing the impact of altered circuit behavior on the physiology of recorded neurons. In addition, deletion of AMPAR subunit alleles occurred in closer temporal relation to the time of recording than can be achieved in germline mutants, reducing possible compensatory effects. Simultaneous recordings from a GFP-expressing cell and a neighboring control cell, with a single stimulating electrode to evoke EPSCs in both cells, permitted study of the postsynaptic effects of the genetic manipulation while controlling for presynaptic inputs.

By breeding the *GRIA1*$^{fl/fl}$, *GRIA2*$^{fl/fl}$, and *GRIA3*$^{fl/fl}$ mice to each other, we succeeded in generating triple-*GRIA1-3*$^{fl/fl}$ mice. Figure 2A shows a typical acute slice made at P25 from a mouse injected at P0 with CA1 pyramidal cells infected with rAAV-Cre-GFP. Cre expression, and thus GFP, is confined to the nucleus. Recording from a Cre-expressing cell (green trace in inset) in the triple-*GRIA1-3*$^{fl/fl}$ mice demonstrated the complete absence of AMPAR EPSCs recorded at −70 mV (Figures 2B1 and 2B3), whereas the size of the NMDAR EPSCs was the same as that recorded in the control cell (black trace in inset) (Figures 2B2 and 2B3). We also measured the glutamate-evoked AMPAR currents from extrasynaptic receptors in somatic OOPs. In contrast to the large and reproducible currents in control cells, Cre-expressing cells exhibited no detectable current (Figure 2C). These findings indicate that GluA1, -A2, and -A3 fully account for functional AMPARs in CA1 pyramidal cells. In no case did Cre-expressing cells express AMPARs, indicating that the recombination is extremely efficient.

The lack of change in the NMDAR EPSCs suggests that the number of synapses and release of glutamate are unchanged. We examined the properties of the NMDAR EPSCs more closely, because it is well established that neuronal activity controls the developmental switch of the subunit composition of synaptic NMDARs (Barria and Malinow, 2002; Bellone and Nicoll, 2007; Carmignoto and Vicini, 1992; Philpot et al., 2001). In particular, immature synapses primarily express NR2B-containing receptors with slow kinetics and high sensitivity to the NR2B-selective antagonist ifenprodil. These receptors are then replaced by NR2A-containing receptors with fast kinetics. Surprisingly, despite the loss of all AMPAR excitatory drive, the decay of the NMDAR EPSCs (Figure 2D), as well as their sensitivity to ifenprodil (Figures 2E1 and 2E2), were the same as in control cells, indicating that neuronal activity, presumably due to NMDAR activation in these cells in vivo, is still sufficient for the "activity-dependent" switch in NR2 subunits observed during development. Finally, we examined the voltage sensitivity of the NMDAR EPSCs and found that it, too, was the same as that in control cells (Figure 2F).

The lack of change in the NMDAR EPSCs implies that there is no change in the number of synapses or in the release of glutamate in our experimental conditions. A detailed examination of the morphology of neurons entirely lacking AMPARs confirmed the physiological results. After about 3 weeks of rAAV-Cre-GFP injection, when the infected neurons lack detectable AMPAR-mediated currents (Figures 2B and 2C), CA1 pyramidal neurons were filled with fluorescent dyes, fixed, and examined with confocal microscopy (Figures 2G and 2H). We could detect no change in the average number of branchpoints of dendrites, dendritic length, or spine density (see the Experimental Procedures).

Synaptic Transmission Is Mediated Primarily by GluA1A2 Heteromeric Receptors

Given that surface AMPAR expression does not exist after GluA1, -A2, and -A3 deletion, we next sought to determine the relative contributions of each subunit. We first examined the consequence of deleting GluA1 over time. Organotypic hippocampal slice cultures provided a simple preparation to follow the time course of subunit depletion. We prepared slice cultures from P5-7 mice (see the Experimental Procedures) and performed biolistic transfection of a Cre-IRES-GFP construct 2 days later. Following the expression of Cre in *GRIA1*$^{fl/fl}$ hippocampal slice cultures, there was a gradual decrease in AMPAR EPSC amplitudes that stabilized at ~20% of control values at ~14 days after transfection, while there was no change in the NMDAR EPSCs (Figures 3A1 and 3A2). None of the manipulations carried out in the rest of this study resulted in a change in the NMDAR EPSC. Although a precise time course was not carried out in the P0 in vivo inoculation experiments, AMPAR EPSCs also stabilized at ~20% but required approximately

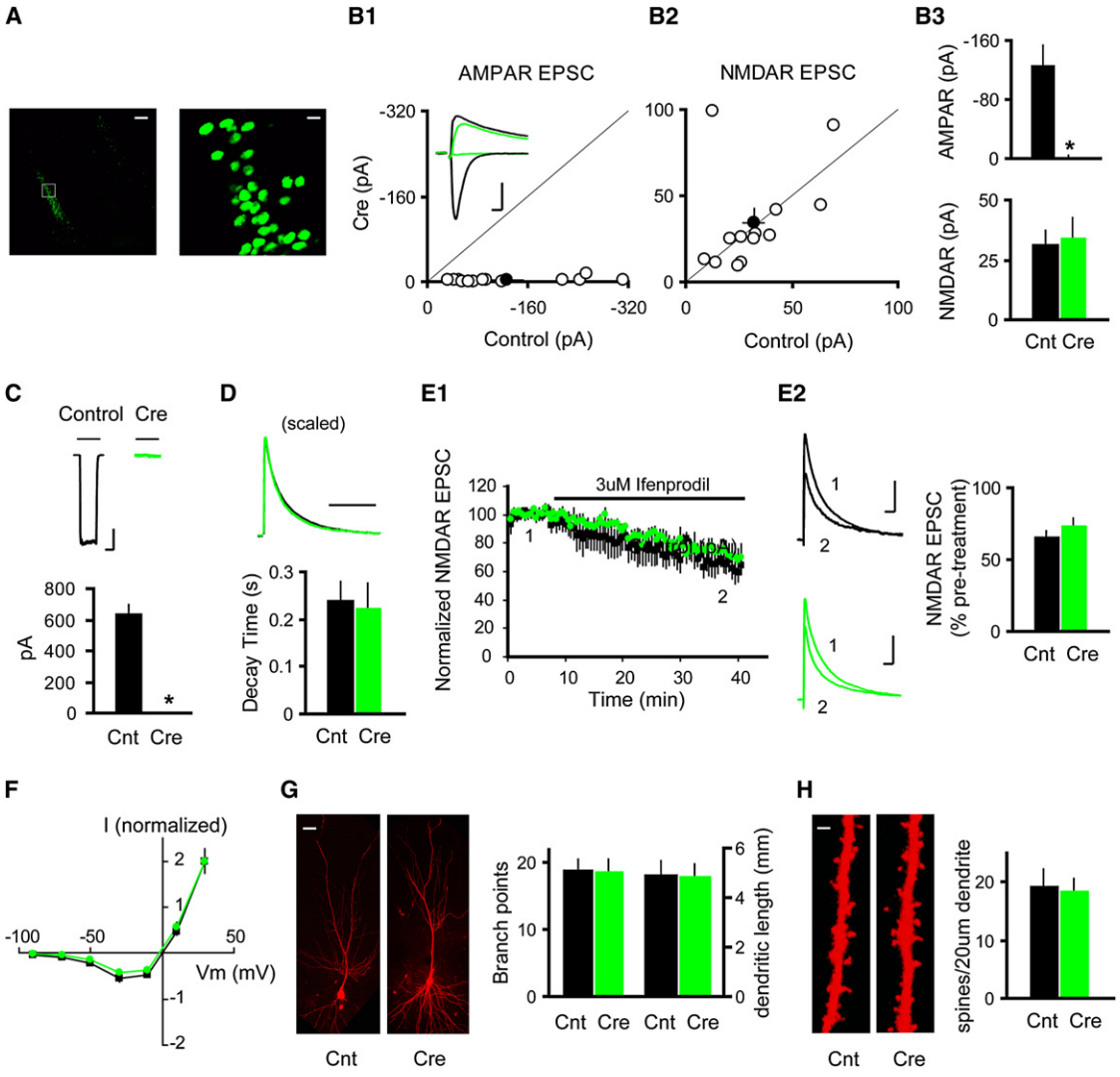

Figure 2. Synaptic Physiology and Morphology of CA1 Pyramidal Neurons without AMPARs

(A) Confocal images (left, low magnification; right, high magnification of the boxed area in left) show mosaic expression of Cre-GFP in the CA1 region of a typical hippocampal acute slice made from a triple-*GRIAX*$^{fl/fl}$ mouse at P25 injected at P0 with rAAV-Cre-GFP. Scale bar, left, 0.2 mm; right, 20 μm.

(B) Scatter plots show amplitudes of EPSCs for single pairs (open circles) and mean ± SEM (filled circles), respectively. The scatter plots represented the data recorded from acute slices (P22–P30) infected with rAAV-CRE-GFP at P0. Distributions of EPSC amplitudes show a virtual elimination of AMPAR EPSCs (B1, Control [Cnt], −127.1 ± 26.6 pA; Cre, −3.1 ± 1.0 pA; n = 13; *p < 0.001) but no change in NMDAR EPSCs (B2, control, 32.0 ± 5.1 pA; Cre, 34.7 ± 8.0 pA, n = 13; p = 0.73). (Inset in B1) Sample traces are as follows: black, control cell; green, Cre cell. (B3) Bar graph shows average AMPAR (top) and NMDAR (bottom) EPSCs presented in (B1 and B2).

(C) Traces of glutamate-evoked currents from OOPs in control (black) and Cre cells (green). Bar graph shows that deletion of GluA1, -A2, and -A3 eliminated the AMPAR-mediated current (Cnt, −648.7 ± 45.2 pA; n = 23; Cre, −1.0 ± 0.7 pA; n = 8; *p < 0.001). Scale bar, 200 pA, 1 s.

(D) Bar graph shows the decay time constant of NMDAR EPSCs recorded in NBQX at +40 mV (Cnt, 0.24 ± 0.01 s, n = 22; Cre, 0.23 ± 0.01 s, n = 24; p > 0.05). Scale bar, 0.5 s.

(E) (E1 and E2) Ifenprodil (3 μM) depressed NMDAR EPSCs recorded at +40 mV in Cnt and Cre cells to a similar extent. (E2) Traces of NMDAR EPSCs from the two groups of cells before and 30 min after ifenprodil application were shown on the right. Bar graph shows the average percentage of NMDAR EPSCs remaining after ifenprodil application (Cnt, 66.8% ± 3.7%, n = 4; Cre, 74% ± 4.8%, n = 5; p > 0.05). Scale bar, 50 pA, 0.1 s.

(F) I/Vs of synaptic NMDARs. NMDAR EPSCs were recorded at various holding potentials (−80, −60, −40, −20, 0, +20, and +40 mV) with 4 mM Mg^{2+}. Junction potentials have been corrected.

(G) Representative confocal stacks from Cnt and Cre cells. Bar graph in right shows average number of dendritic branchpoints and dendritic length (Cnt, n = 10; Cre, n = 8; p > 0.05). Scale bar, 20 μm.

(H) Representative confocal stacks of 20 μm secondary apical dendrites from Cnt and Cre cells. Bar graph in right shows average spine density (Cnt, n = 11; Cre, n = 11; p > 0.05). Scale bar, 2 μm.

(A–H) The recordings and anatomy were made from acute slices (P20–P30) from animals injected at P0 with rAAV-Cre-GFP.

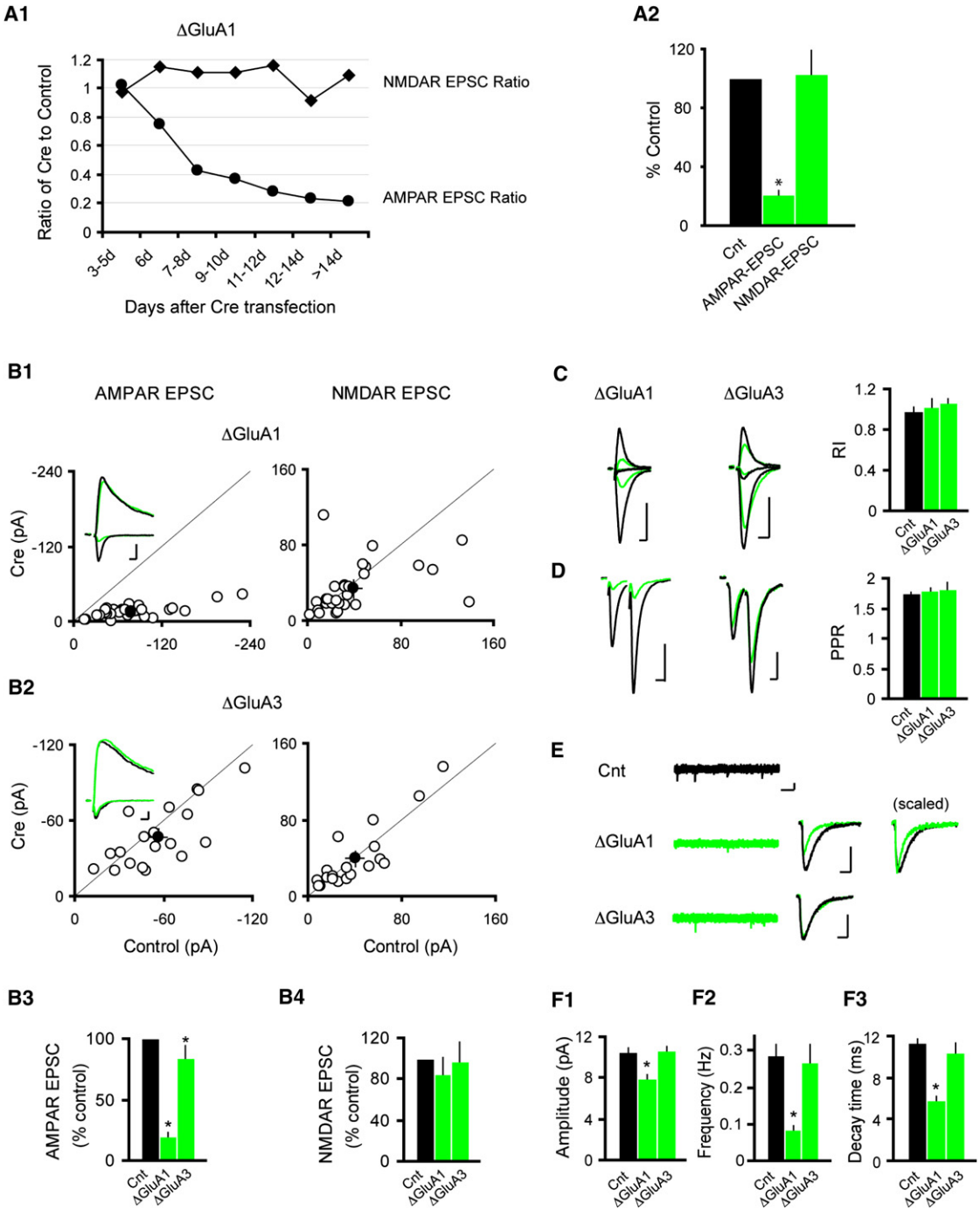

Figure 3. Excitatory Synaptic Transmission at CA1 Pyramidal Neurons Is Mediated Primarily by GluA1A2 Heteromers

(A) (A1 and A2) The time course for changes in AMPAR EPSCs in hippocampal slice cultures from *GRIA1*$^{fl/fl}$ mice after transfection of Cre-IRES-GFP. For ΔGluA1, shown are the ratio of AMPAR-EPSCs (closed circles, 3–5 days, 1.02; 6 days, 0.75; 7–8 days, 0.43; 9–10 days, 0.37; 11–12 days, 0.28; 12–14 days, 0.23; >14 days, 0.21) and ratio of NMDAR-EPSCs (closed diamonds, 3–5 days, 0.98; 6 days, 1.15; 7–8 days, 1.11; 9–10 days, 1.11; 11–12 days, 1.16; 12–14 days, 0.92; >14 days, 1.09) from transfected cells to neighboring control cells, respectively. (A2) Bar graph shows the percentage of AMPAR EPSCs (21.2% ± 3.1%; n = 15; *p < 0.0001) and NMDAR EPSCs (104.8% ± 17.6%; n = 14; p = 0.53) to controls.

(B) (B1–B4) Scatter plots (B1 and B2) and bar graphs (B3 and B4) show amplitudes of EPSCs for single pairs (open circles) and mean ± SEM (filled circles) for *GRIA1*$^{fl/fl}$ (B1, pooled data from acute slices [P19–P24] from animals injected at P0–P2 and from hippocampal slice cultures) and *GRIA3*$^{fl/fl}$ (B2, data from acute slices [P20-P25] from animals injected at P0–P2), respectively. (Inset in B1 and B2) Sample traces are as follows: black, control; green, Cre. (B3) EPSC amplitudes show a significant reduction in AMPAR EPSCs for the deletion of either subunit (ΔGluA1, Cnt, −77.7 ± 12.7 pA; Cre, −15.1 ± 2.4 pA; n = 31, *p < 0.0001; ΔGluA3,

3 weeks after initial viral injection to reach this stabilized state. Since there was no obvious difference between the two sets of data (see Figure S1 available online), we pooled the data from both slice cultures and acute slices for each pair of recordings. The scatter plot shows that there was an 80.6% ± 3.1% (n = 31) loss of the AMPAR EPSCs (Figures 3B1, 3B3, and 3B4). The I/V of the remaining AMPAR EPSCs, recorded after pharmacological blockade of NMDARs, remained linear, indicating that the remaining receptors contained GluA2 (Figure 3C). To analyze the mechanism for reduced AMPAR EPSCs, we recorded mEPSCs (Figures 3E and 3F). There was a clear decrease in the amplitude of mEPSCs (Figure 3F1), indicating that there is a loss of AMPARs from all synapses, as well as a decrease in frequency (Figure 3F2). Given the absence of any apparent change in presynaptic release probability, as measured by PPF (Figure 3D), a decrease in mEPSC frequency could be explained if functional AMPARs at a population of synapses are below the detection threshold or lost entirely. As the decay kinetics of mEPSCs depends on subunit composition (Jonas, 2000), we measured the decay of mEPSCs. Superimposed peak-normalized traces (Figure 3E) show that the kinetics are faster in the absence of GluA1 (Cnt, 11.3 ± 0.5 ms, n = 22; GluA1, 7.7 ± 1.4 ms, n = 10; $p < 0.01$) (Figure 3F3). These data suggest that GluA1A2 heteromers account for approximately 80% of synaptic AMPARs. Although there remains the formal possibility that some GluR1 protein persists weeks after the onset of Cre expression, and that remaining AMPARs still contain GluA1, it is more likely that remaining AMPARs are GluA2A3 heteromers, as demonstrated below.

The profound loss of functional synaptic AMPARs following the ablation of GluA1, coupled with the fact that the I/V of the synaptic currents remains linear, suggests that GluA2A3 receptors contribute ~20% to basal synaptic transmission. In keeping with the modest role of GluA3, deleting GluA3 resulted in a 16.3% ± 10.0% (n = 19) decrease in AMPAR EPSCs (Figures 3B2 and 3B3). It remains a possibility that some type of compensation might underestimate the actual contribution of GluA3. However, the cross-validation by deletion of GluA1 or GluA3 alone (Figure 3B) suggests that such compensation, if any, is minimal. Given the small effects of GluA3 deletion, we did not examine time points earlier than 3 weeks after rAAV-Cre-GFP infection. The change in synaptic transmission was not associated with any change in rectification (Figure 3C) or in PPF (Figure 3D). No significant change in either the amplitude or the frequency of mEPSCs was detected (Figures 3E and 3F). These data suggest that about 80% of receptors are GluA1A2 heteromers and that about 16% are GluA2A3 heteromers at excitatory synapses of CA1 pyramidal neurons.

Synaptic AMPARs Adapt Rapidly to the Deletion of GluA2

Since all surface AMPARs in CA1 pyramidal neurons contain GluA2, we were interested in how the cell responded to its loss. Following the transfection of Cre in slice cultures, the AMPAR EPSC amplitudes fell to ~50% of control values at 6 days and then remained constant (Figure 4A1). In contrast, there was a gradual decrease in the rectification index (RI), measured in the presence of NMDAR blockers, which stabilized at 12–14 days (Figures 4A1, 4A2, and 4C). It is not entirely clear what might account for the striking difference in the rectification and AMPAR-mediated EPSC amplitude at day 6. Nevertheless, the decrease in RI represents the gradual loss of GluA2-containing receptors. The RI at 12–14 days is identical to that recorded in the GluA2 germline KO, indicating that by 2 weeks no functional GluA2-containing synaptic receptors are left (Figures 4A1 and 4A2). In these same experiments, no change in the NMDAR EPSCs was observed (Figures 4A1 and 4A2). rAAV-Cre-GFP experiments with *GRIA2*$^{fl/fl}$ mice also showed that loss of GluA2 caused an ~50% loss of AMPAR EPSCs. Since there was no obvious difference between the results obtained from P0 injections and the slice culture experiments (Figure S1), the data were pooled, and a single scatter plot of the values obtained at 12–14 days postinfection/posttransfection is shown (Figures 4B1–4B3). There was a 48.3% ± 3.8% (n = 86) loss of the AMPAR EPSCs. In addition, PPF did not change, excluding a change in release probability (Figure 4D).

Is the decrease in the evoked synaptic responses due to a uniform loss of receptors across the entire population of synapses, as in the case with GluA1 deletion? To address this question, we examined mEPSCs (Figures 4E and 4F). Remarkably, there was no change in the mean amplitude of mEPSCs (Figures 4E and 4F1) but a dramatic reduction in frequency (Figure 4F2). This suggests that two processes occur during the loss of GluA2; approximately half of the synapses become devoid of AMPARs, while in the other half of synapses, GluA2-containing receptors are gradually replaced by GluA2-lacking receptors. This implies that there are two distinct populations of synapses, based on whether they can recruit GluA2-lacking receptors. We also examined the decay kinetics of the mEPSCs and found no difference between control cells and GluA2-lacking cells (Figure 4F3).

All Subunits Form Homomeric Receptors, which Traffic to Synapses in Double GluA Deletions

Since deletion of all three subunits abolishes AMPAR EPSCs, transmission recorded in the absence of any two subunits is presumably generated by homomeric receptors composed of

Cnt, −56.4 ± 6.0 pA; Cre, −47.2 ± 5.6 pA; n = 19; *$p < 0.05$). (B4) There was no change in the NMDAR EPSCs (GluA1, Cnt, 40.0 ± 9.4 pA; Cre, 33.6 ± 6.9 pA, n = 29; p = 0.31; ΔGluA3, Cnt, 40.4 ± 7.7 pA; Cre, 39.0 ± 7.8 pA, n = 19; p = 0.97).

(C and D) Bar graphs show average RI (C) (Cnt, 0.99 ± 0.03, n = 30; ΔGluA1, 1.02 ± 0.08, n = 14; p = 0.63; ΔGluA3, 1.06 ± 0.04, n = 15; p = 0.15) and average paired-pulse ratio (PPR, [D]) (Cnt, n = 84; ΔGluA1, n = 40; ΔGluA3, n = 9; $p > 0.05$ for both conditions). Left were sample traces.

(E) Sample traces of mEPSCs shown at a low gain and sweep speed (traces on left; scale bar, 10 pA, 500 ms) and averaged mEPSCs at a high gain and sweep speed (traces on right). Control trace (black) has been superimposed on the trace from a Cre cell. Scale bar, 5 pA, 10 ms. mEPSCs were recorded from acute hippocampal slices (P20–P27) from animals injected at P0–P2.

(F) (F1) Bar graphs show mEPSC amplitude (Cnt, −10.5 ± 0.4 pA; ΔGluA1, −7.9 ± 0.5 pA; *$p < 0.001$; ΔGluA3, −10.7 ± 0.1 pA; p = 0.77), (F2) frequency (Cnt, 0.28 ± 0.03 Hz; ΔGluA1, 0.08 ± 0.01 Hz; p* < 0.001; ΔGluA3, 0.27 ± 0.05 Hz, p = 0.68), and (F3) decay (Cnt, 11.30 ± 0.49 ms; ΔGluA1, 7.73 ± 1.41 ms; *$p < 0.01$; ΔGluA3, 11.60 ± 1.20 ms; p = 0.81). n = 22, 10, and 20 for Cnt, ΔGluA1, and ΔGluA3, respectively.

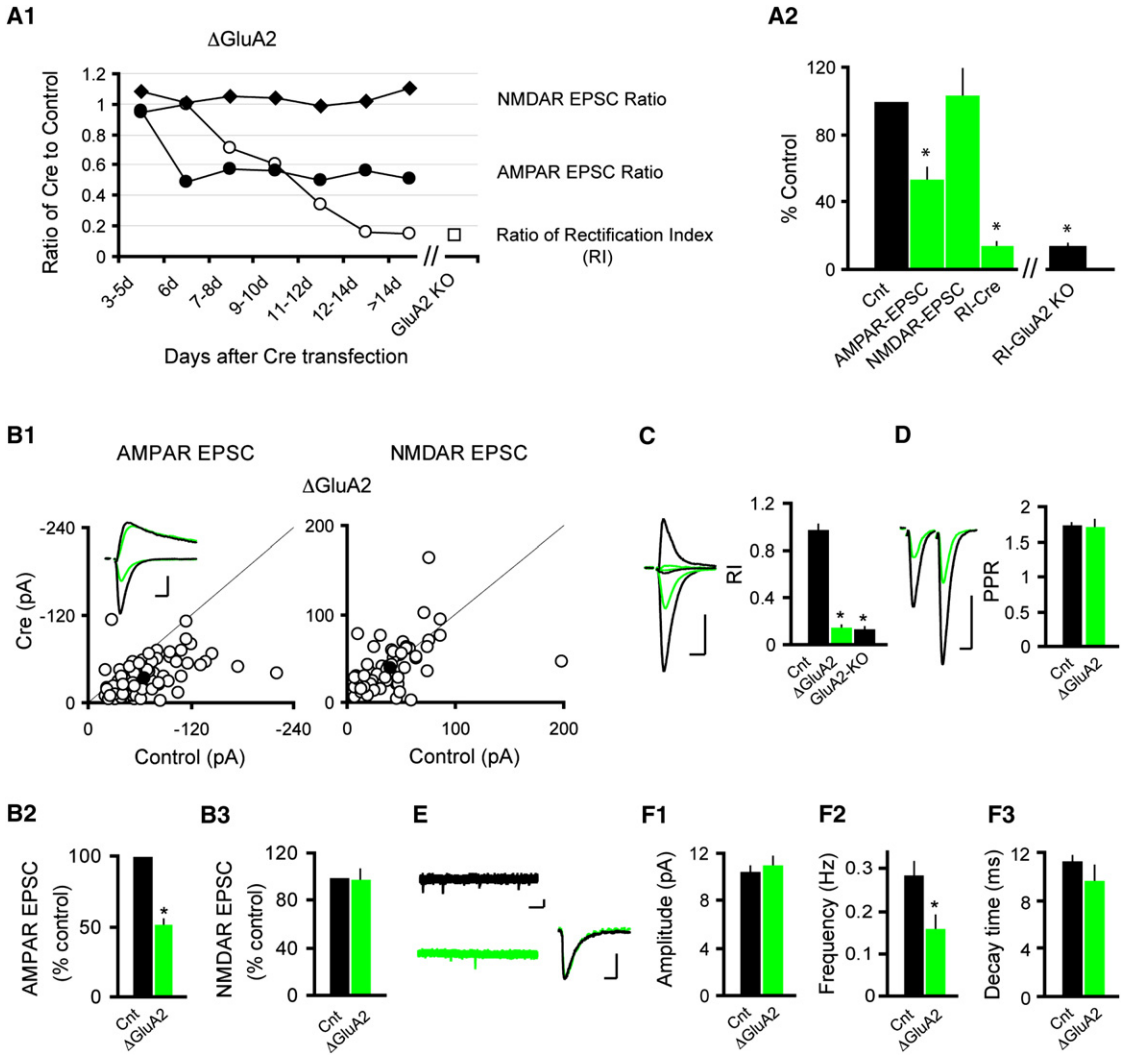

Figure 4. AMPARs Adjust Rapidly to the Deletion of GluA2

(A) (A1 and A2) The time course for the changes in synaptic transmission in hippocampal slice cultures from *GRIA2*$^{fl/fl}$ mice after transfection of Cre-IRES-GFP. Ratio of RI (open circles, 3–5 days, 0.95; 6 days, 0.99; 7–8 days, 0.71; 9–10 days, 0.60; 11–12 days, 0.34; 12–14 days, 0.16; >14 days, 0.15), ratio of AMPAR EPSCs (closed circle, 3–5 days, 0.96; 6 days, 0.49; 7–8 days, 0.57; 9–10 days, 0.56; 11–12 days, 0.50; 12–14 days, 0.57; >14 days, 0.51), and ratio of NMDAR EPSCs (closed diamonds, 3–5 days, 1.08; 6 days, 1.01; 7–8 days, 1.06; 9–10 days, 1.04; 11–12 days, 0.99; 12–14 days, 1.01; >14 days, 1.10) from transfected cells to neighboring control cells, respectively. Open square shows RI from CA1 pyramidal neurons from germline GluA2 KO mice (0.13 ± 0.02, n = 5). (A2) Graph shows the percentage of the average AMPAR EPSCs (51.7% ± 5.2%; n = 86; *p < 0.0001), NMDAR EPSCs (97.8% ± 13.2%; n = 64; p = 0.81), and RI (15.0% ± 1.8%; n = 19; *p < 0.0001) from transfected cells or GluA2 KO cells (13.3% ± 2.0%; n = 5; *p < 0.01) to control cells.

(B) (B1–B3) Scatter plots (B1) and bar graphs (B2 and B3) show amplitudes of EPSCs for single pairs (open circles) and mean ± SEM (filled circles) for *GRIA2*$^{fl/fl}$. (Inset in B1) Sample traces are as follows: black, control; green, Cre. (B2) EPSC amplitudes show a significant reduction in the AMPAR EPSCs (Cnt, −66.2 ± 3.8 pA; Cre, −34.2 ± 2.5 pA; n = 86; *p < 0.0001). (B3) There was no change in the NMDAR EPSCs (GluA2, Cnt, 40.0 ± 3.7 pA; Cre, 39.1 ± 3.4 pA, n = 64; p = 0.81). The data were pooled from acute hippocampal slices (P13–P17) from animals injected at P0–P2 and from hippocampal slice cultures.

(C and D) Bar graphs show average RI (C) (Cnt, 0.99 ± 0.03, n = 30; ΔGluA2, 0.15 ± 0.02, n = 19; *p < 0.001) and average PPR (D) (Cnt, n = 84; ΔGluA2, n = 29; p > 0.05). Left were sample traces.

(E) Sample traces of mEPSCs shown at a low gain and sweep speed (traces on left; scale bar, 10 pA, 500 ms) and averaged mEPSCs at a high gain and sweep speed (traces on right). Control trace (black) has been superimposed on the trace from a Cre cell. Scale bar, 5 pA, 10 ms. mEPSCs were recorded from acute hippocampal slices (P13–P18) from animals injected at P0–P2.

(F) (F1) Bar graphs show mEPSCs amplitude (Cnt, −10.51 ± 0.37 pA; ΔGluA2, 11.08 ± 0.65 pA; p = 0.42), (F2) frequency (Cnt, 0.28 ± 0.03 Hz; ΔGluA2, 0.16 ± 0.03 Hz; *p < 0.001), and (F3) decay (Cnt, 11.30 ± 0.49 ms; ΔGluA2, 9.75 ± 1.14 ms; p = 0.27). n = 22 and 17 for Cnt and ΔGluA2, respectively.

the remaining subunit. The combined deletion of both GluA2 and -A3 caused a 57.2% ± 5.2% (n = 14) reduction in the amplitude of the AMPAR EPSCs (Figures 5A1 and 5A4). As expected from the deletion of GluA2, the rectification of the remaining AMPAR EPSCs in the combined deletion was strongly rectifying (Figure 5B). There was no change in PPF (Figure 5C). We also

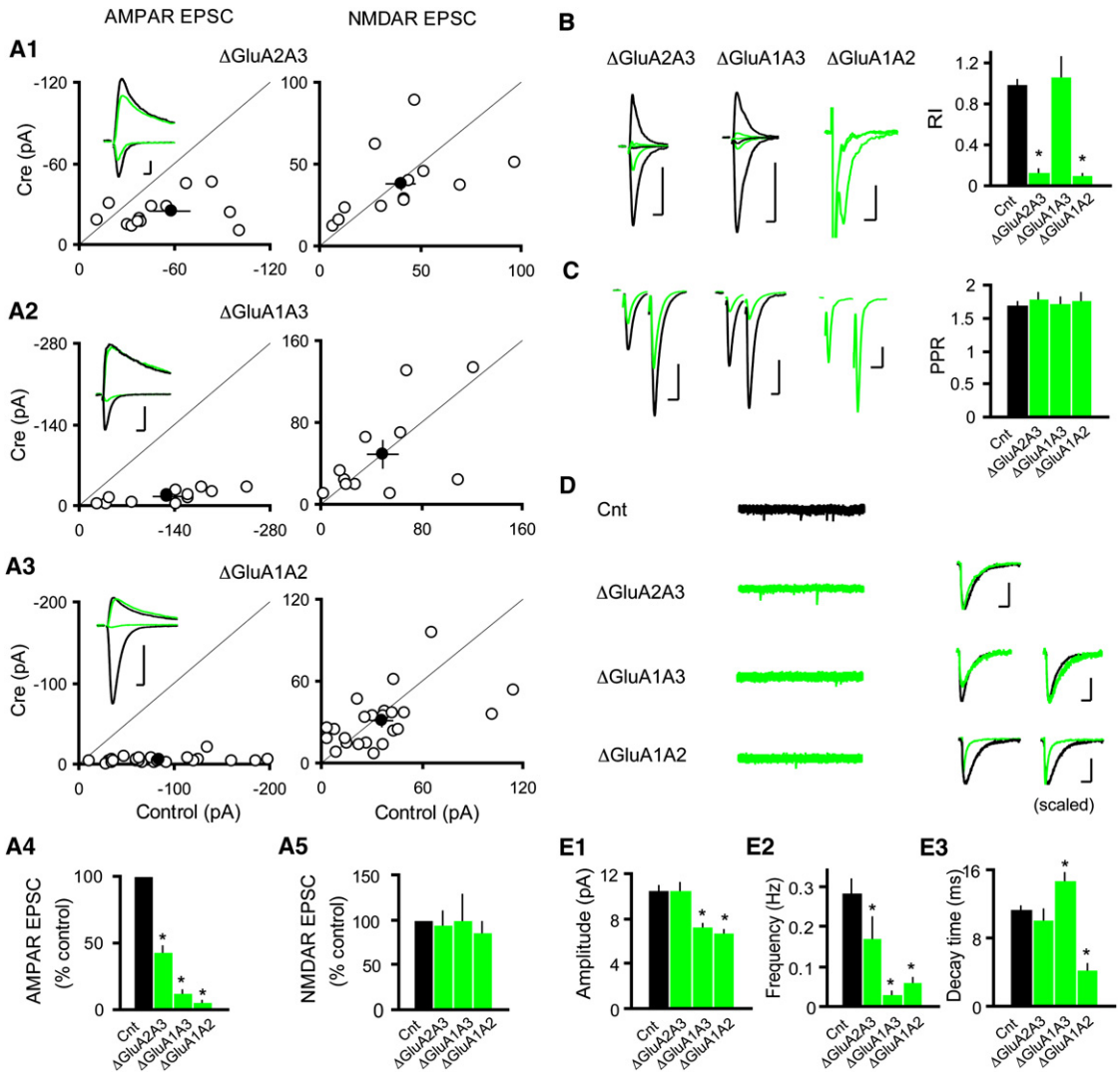

Figure 5. Deletion of GluA2A3, GluA1A3, or GluA1A2 in CA1 Pyramidal Cells

(A) (A1–A5) Scatter plots (A1–A3) and bar graphs (A4 and A5) show amplitudes of EPSCs for single pairs (open circles) and mean ± SEM (filled circles) for *GRIA2A3*$^{fl/fl}$ (A1), *GRIA1A3*$^{fl/fl}$ (A2), and *GRIA1A2*$^{fl/fl}$ (A3), respectively. (A4) The amplitudes of AMPAR EPSCs were significantly reduced in all three cases (ΔGluA2A3, Cnt, −58.1 ± 11.4 pA; Cre, −24.9 ± 3.3 pA; n = 14; *p < 0.01; ΔGluA1A3, Cnt, −128.4 ± 19.7 pA; Cre, −15.6 ± 3.10 pA; n = 12; *p < 0.001; ΔGluA1A2, Cnt, −84.3 ± 10.1 pA; Cre, −4.9 ± 0.8 pA; n = 24; *p < 0.001). (A5) No change in the size of NMDAR EPSCs was observed (ΔGluA2A3, Cnt, 40.3 ± 7.4 pA; Cre, 38.0 ± 6.3 pA, n = 12; p = 0.82; ΔGluA1A3, Cnt, 49.2 ± 11.7 pA; Cre, 49.0 ± 13.7 pA, n = 11; p = 0.99; ΔGluA1A2; Cnt, 36.3 ± 5.8 pA; Cre, 31.0 ± 4.2 pA, n = 23; p = 0.31). (Inset in A1–A3) Sample traces are as follows: black, control; green, Cre.

(B and C) Bar graphs show average RI (B) (Cnt, 0.99 ± 0.03, n = 30; ΔGluA2A3, 0.14 ± 0.02, n = 13; *p < 0.001; ΔGluA1A3, 1.06 ± 0.2, n = 5; p = 0.59; ΔGluA1A2, 0.1 ± 0.02, n = 6; *p < 0.001) and average PPR (C) (Cnt, n = 84; ΔGluA2A3, n = 14; ΔGluA1A3, n = 6; ΔGluA1A2, n = 11; p > 0.05 for each conditions). Left were sample traces. For *GRIA1A2*$^{fl/fl}$ cells, the stimulus was increased to record measurable EPSCs, and only recordings from the Cre cell were shown.

(D) Sample recordings of mEPSCs at low gain and sweep speed (traces on left; scale bar, 10 pA, 500 ms) and averaged mEPSCs at high gain and sweep speed (traces on right). Control trace (black) has been superimposed on the trace from a Cre cell. Scale bar, 5 pA, 10 ms.

(E) (E1) Bar graphs show mEPSC amplitude (top, Cnt, −10.51 ± 0.37 pA; ΔGluA2A3, −10.56 ± 0.60 pA; p = 0.93; ΔGluA1A3, −7.21 ± 0.36 pA; *p < 0.001; ΔGluA1A2, −6.79 ± 0.20 pA; *p < 0.001), (E2) frequency (middle, Cnt, 0.28 ± 0.03 Hz; ΔGluA2A3, 0.17 ± 0.05 Hz; *p < 0.005; ΔGluA1A3, 0.03 ± 0.01 Hz; *p < 0.001; ΔGluA1A2, 0.06 ± 0.01 Hz, *p < 0.001), and (E3) decay (bottom, Cnt, 11.30 ± 0.49 ms; ΔGluA2A3, 10.18 ± 1.2 ms; p = 0.33; ΔGluA1A3, 14.70 ± 0.71 ms; *p < 0.01; ΔGluA1A2, 4.20 ± 0.71 ms; *p < 0.001). n = 22, 14, 7, and 9 for Cnt, ΔGluA2A3, ΔGluA1A3, and ΔGluA1A2, respectively.

(A–E) The recordings were made from acute hippocampal slices (P20–P27) from animals injected at P0–P1.

examined the consequence of deleting GluA2A3 on the properties of mEPSCs (Figures 5D and 5E). The results were similar to those for the *GRIA2*$^{fl/fl}$, suggesting that there is an all-or-none silencing of a population of excitatory synapses. Given the small effect of deleting GluA3 on glutamate-mediated responses in CA1 pyramidal cells, it is not surprising that the combined deletion of GluA2 and -A3 had a similar impact to that of just deleting GluA2, again emphasizing the modest contribution of GluA2A3

receptors to basal synaptic transmission. It also suggests that the receptors remaining in the GluA2-deleted neurons are essentially all GluA1 homomers, with little evidence for the contribution of GluA1A3 heteromers.

The GluA1A3 double KO is a particularly interesting one because there is uncertainty concerning the ability of edited GluA2 subunits to form functional homomeric receptors in neurons. It has long been known that edited GluA2 subunits, unlike other subunits, produce very small currents as homomeric channels in heterologous expression systems (Burnashev et al., 1992; Hollmann and Heinemann, 1994). Although deletion of both GluA1 and -A3 reduced the AMPAR EPSCs to a greater extent than did the GluA1 deletion alone, there was still 12.1% ± 2.4% (n = 12) of the AMPAR EPSCs remaining after 3 weeks of virus injection (Figures 5A2 and 5A4). The remaining current was most likely generated by synaptic GluA2 homomers, since in the triple KO no AMPAR EPSCs were left at the similar time point after virus injection (Figure 2B1) and it was blocked by 100 μM GYKI, an AMPAR-selective antagonist (n = 3, data not shown). Interestingly, the I/V of the remaining EPSC was linear (Figure 5B), indicating that the trafficked GluA2 receptors are edited. Analysis of mEPSCs indicated a modest decrease in amplitude (Figures 5D and 5E1) and a dramatic decrease in frequency (Figure 5E2). The decay of mEPSCs was actually slower (Cnt, 11.3 ± 0.5 ms, n = 22; GluA1A3, 14.7 ± 0.9 ms, n = 7; $p < 0.005$) than that of control cells (Figure 5E3). These results indicate that, in the absence of other subunits, GluA2 can form homomers that traffic to a few synapses. However, the process is very inefficient at maintaining synaptic transmission.

Finally we examined the consequence of deleting both GluA1 and -A2. This resulted in a 94.5% ± 1.4% (n = 24) loss of AMPAR EPSCs (Figures 5A3 and 5A4), which was statistically greater than the loss from the GluA1 deletion, further establishing the dominant role of GluA1A2 heteromers in excitatory synaptic transmission onto CA1 pyramidal cells. As in the case of GluA1 deletion, the amplitude (Figures 5D and 5E1) and the frequency (Figures 5D and 5E2) of the mEPSCs were strongly reduced. Furthermore, the decay of the mEPSCs (4.2 ± 0.7 ms, n = 9; $p < 0.005$) was extremely fast (Figures 5D and 5E3). Since no AMPAR EPSCs remain in the triple KO, we presume that the remaining EPSCs in the GluA1A2 KO are mediated by homomeric GluA3 receptors. To examine the properties of the remaining EPSC, we increased the stimulus strength to record measurable EPSCs in cells expressing Cre. The remaining EPSCs were highly rectifying (Figure 5B), indicating absence of GluA2-containing AMPARs. The remaining receptors could be residual GluA1 subunits that form either homomeric GluA1 receptors or GluA1A3 heteromers. However, the fact that mEPSCs generated in the GluA1A2 double KO cells (Figures 5D and 5E3) were considerably faster than those generated by GluA1 homomeric receptors (those recorded in the GluA2A3 double KO cells) (10.2 ± 1.2 ms, n = 14) supports a model in which GluA3 receptors can assemble as homomers and traffic to synapses when GluA1 and -A2 subunits are absent. However, such aberrant assemblies are unlikely to contribute to synaptic transmission in WT neurons, as essentially all synaptic AMPARs contain GluA2 in CA1 pyramidal neurons.

The Contribution of AMPAR Subunits to Extrasynaptic AMPARs

Glutamate application to somatic OOPs from control CA1 pyramidal neurons indicates that AMPARs are abundant in extrasynaptic membranes (Figures 1, 2C, 6A, and 6C). This extrasynaptic population of AMPARs has been proposed to be a reserve pool for synapses (Adesnik et al., 2005) and may undergo dynamic exchange with synaptic population of AMPARs (Bats et al., 2007). It should be emphasized that, although somatic AMPARs are clearly extrasynaptic, they may not be identical to dendritic extrasynaptic receptors. However, at least for the GluA1 conventional KO, there is the same loss of receptors from the soma and from the extrasynaptic dendritic shaft (Andrasfalvy et al., 2003), suggesting that AMPARs at somatic and dendritic extrasynaptic membranes are similar. With these caveats, we sought to determine the subunit composition of these somatic extrasynaptic AMPARs. Simultaneous deletion of all subunits abolished extrasynaptic receptors (Figure 2C). Deletion of GluA1 resulted in a 94.7% ± 7.1% (n = 16) loss of these receptors (Figures 6A and 6B). The I/V of the remaining current was linear (Figure 6B), indicating that the remaining receptors are primarily GluA2A3 heteromers. Compared to the profound loss of extrasynaptic current (~95%), synaptic currents were less impaired (~80%) in GluA1-deleted cells (Figure 6D), suggesting that synapses are capable of consolidating the few remaining GluA2A3 heteromers. Surprisingly, there was no change in the glutamate-evoked currents measured at −70 mV in patches from GluA2-lacking cells (Figures 6A and 6B). However, based on the strong inward rectification of the responses (Figure 6B), it is clear that GluA2-lacking receptors fully account for the currents. The fact that the size of the extrasynaptic currents is unchanged is of considerable interest in the context of the reduction in the evoked EPSCs (Figure 6C). This suggests a critical role for the GluA2 subunit in transferring extrasynaptic receptors to the synapse. This notion is all the more striking when one considers the all-or-none loss of mEPSCs upon deleting GluA2, which implies that one population of synapses requires the presence of GluA2 for any AMPAR trafficking, while another population does not. Such heterogeneity adds considerably to the complexity of AMPAR trafficking. Currents in patches from GluA3- and GluA2A3-deleted cells were unaltered, whereas those from GluA1A3- and GluA1A2A3-deleted cells were absent (Figures 6A and 6C), emphasizing again the critical role of GluA1 in maintaining extrasynaptic AMPARs. A small amount (24.1 ± 5.2 pA) of extrasynaptic AMPAR-mediated current remained in the OOPs from GluA1A2-deleted cells (Figures 6A and 6C), and the evoked current was rectifying (Figure 6B). These data demonstrated that the majority of extrasynaptic AMPARs (~95%) are GluA1A2 heteromers.

DISCUSSION

The subunit composition of most ionotropic neurotransmitter receptors in the CNS has not been precisely determined. For the AMPA subtype of glutamate receptor, this is a particularly important problem. Recent evidence suggests that the subunit composition of AMPARs determines not only their biophysical properties but their activity-dependent trafficking to the synapse

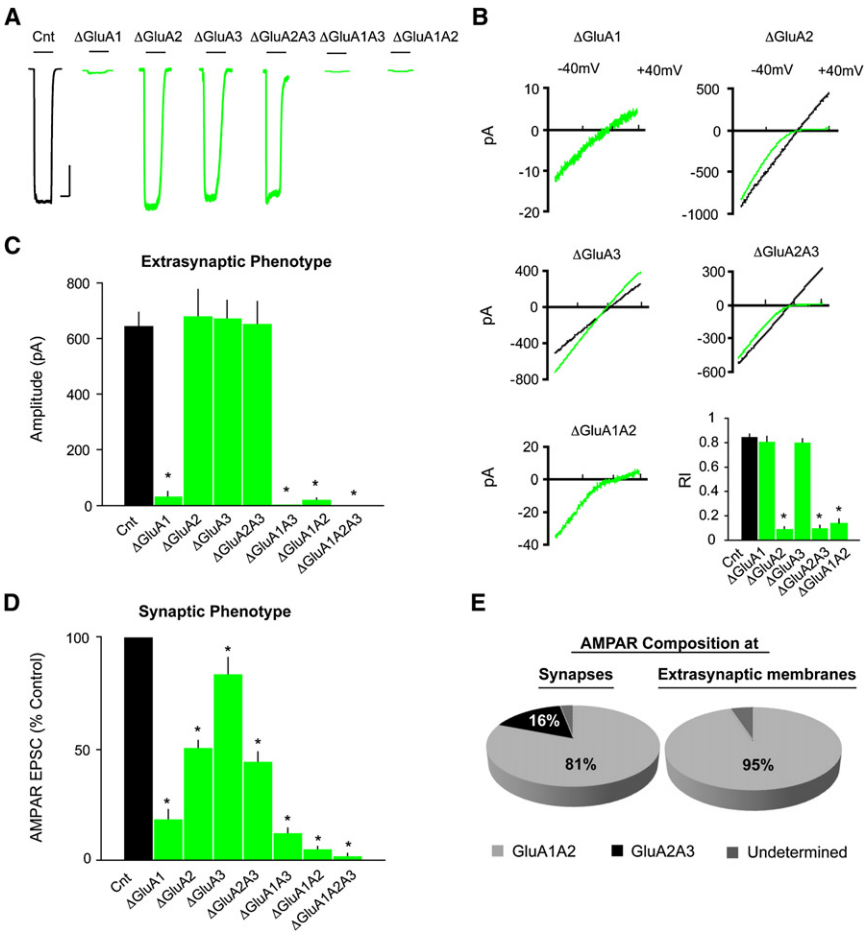

Figure 6. Analysis of Extrasynaptic AMPARs

(A) Sample traces of AMPAR currents from OOPs from uninfected control (black) and Cre (green) cells from CA1 pyramidal neurons from various genetic backgrounds. Scale bar, 200 pA, 1 s. The recordings were made from acute hippocampal slices (P13–P17 for ΔGluA2 and P20–P28 for all other genetic backgrounds) from animals injected at P0–P2.

(B) I/V curves of AMPAR currents from OOPs. Control, black; Cre, green. Deletion of the GluA2 subunit, but not other subunits, caused strong inward rectification of the evoked current. Bar graph at the bottom shows the RI for each condition (Cnt, 0.85 ± 0.02, n = 8; ΔGluA1, 0.81 ± 0.04, n = 5; p = 0.39; ΔGluA2, 0.09 ± 0.01, n = 6; *p < 0.001; ΔGluA3, 0.80 ± 0.03, n = 5; p = 0.22; ΔGluA2A3, 0.10 ± 0.02, n = 6; *p < 0.001; ΔGluA1A2, 0.15 ± 0.03, n = 5; *p < 0.001).

(C) Summary bar graph shows consequences of deletion of respective genes on AMPAR current from OOPs (Cnt, −648.7 ± 45.2 pA, n = 23; ΔGluA1, −35.3 ± 13.1 pA, n = 16, *p < 0.001; ΔGluA2, −684.3 ± 92.2 pA, n = 11, p = 0.70; ΔGluA3, −674.2 ± 63.5 pA, n = 13, p = 0.74; ΔGluA2A3, −656.8 ± 76.3 pA, n = 14, p = 0.92; ΔGluA1A3, −2.5 ± 1.0 pA, n = 14, *p < 0.001; ΔGluA1A2, −24.1 ± 5.2 pA, n = 25, *p < 0.001; ΔGluA1A2A3, −1.01 ± 0.65 pA, n = 8, *p < 0.001).

(D) Summary bar graph shows consequences of deletion of respective genes on AMPAR EPSCs (percent control: ΔGluA1, 19.4 ± 3.1%, n = 31, *p < 0.001; ΔGluA2, 51.7 ± 3.8%, n = 86, *p < 0.001; ΔGluA3, 83.8 ± 1.0%, n = 19, *p < 0.05; ΔGluA2A3, 42.8 ± 5.2%, n = 14, *p < 0.001; ΔGluA1A3, 12.1 ± 2.4%, n = 12, *p < 0.001; ΔGluA1A2, 5.7 ± 1.4%, n = 24, *p < 0.001; ΔGluA1A2A3, 2.4 ± 0.6%, n = 13, *p < 0.001).

(E) Models for AMPAR compositions at synaptic and extrasynaptic membranes. At CA1 pyramidal neurons, ~80% synaptic AMPARs are GluA1A2 heteromers, and ~16% synaptic AMPARs are GluA2A3 heteromers. On the other hand, ~95% extrasynaptic AMPARs are GluA1A2 heteromers.

as well. Thus a rigorous quantitative description of the subunit composition of AMPARs is a prerequisite for understanding their roles in both the maintenance of synaptic transmission and synaptic plasticity. By using a conditional KO approach, we selectively deleted each of the AMPAR subunits, both individually and in combination, in a subset of CA1 hippocampal pyramidal cells. Simultaneous whole-cell recording from a gene-deleted cell and a neighboring control cell was used to quantify the changes induced by these genetic manipulations. The main results of this study are as follows. (1) All surface AMPARs contain GluA2 on CA1 pyramidal neurons. (2) GluA1, GluA2, and GluA3 fully account for the AMPARs on these neurons. (3) About 80% of synaptic AMPARs and >95% of extrasynaptic AMPARs are GluA1A2 heteromers, and most of the remaining receptors are GluA2A3 heteromers. (4) Aberrant homomeric GluA1, GluA2, and GluA3 receptors are capable of forming, depending on the deletion, but are unlikely to contribute significantly to normal AMPAR EPSCs on these neurons. This indicates that there is a hierarchy in the subunit assembly process, with GluA2-containing receptor complexes strongly preferred over other combinations. (5) No detectable changes in NMDAR EPSCs, spine morphology, or presynaptic properties were observed following the removal of all surface AMPARs. As discussed below, these findings provide new insight concerning the roles of AMPARs in neuronal physiology and morphology.

Single-Cell Genetic Approach

We pursued a conditional single-cell genetic approach in an attempt to minimize the contributions of altered circuit behavior or developmental compensation to the observed physiological phenotypes. This was achieved by postnatal in vivo or in vitro expression of Cre recombinase in a small subset of hippocampal CA1 pyramidal neurons from mice homozygous for floxed GluA alleles. To determine the time course for the loss of GluA protein, we monitored AMPAR EPSCs at time points following transfection of Cre. For GluA1 we followed the decline in the size of the AMPAR EPSC, whereas for GluA2 we monitored the change in RI. In both cases, the changes stabilized at approximately 2 weeks following transfection of Cre in slice culture. At this time, the RI in *GRIA2*$^{fl/fl}$ cells was identical to that recorded in the germline KO mice. Notably, although the time course for GluA2 deletion was the same in vitro as in vivo, the deletion of

GluA1 took approximately a week longer in vivo. Possible disparities in the turnover rate of GluA1 in slice cultures compared to the in vivo condition might account for this difference. When considering this time course, it is important to keep in mind that it takes up to a week after injection of Cre virus for recombination to occur in all of the infected cells (Kaspar et al., 2002), reflecting the time necessary to achieve transfection or viral inoculation of the target cells, transcription of the viral vector and expression of the Cre recombinase, and recombination at both allelic chromosomal targets. From that point forward, elimination of the actual protein reflects the half-life of any residual mRNA as well as the half-life of the remaining protein at synaptic and extrasynaptic sites. Given the complexity of this process, it is not surprising that the timing is slightly different in vivo versus in vitro.

One of the clear advantages of the present approach over the germline KO approach is that the neurons do not have to cope with the global absence of the protein throughout their development. However, although Cre-expressing cells in our experiments only experience the full extent of the gene deletion for a few days, it is probably not fair to expect everything else in the neuron to remain absolutely unchanged. Indeed, this is the case for any procedure that involves the knockdown of a protein, most notably, RNAi. What role might compensation play in the present study? In the case of deleting GluA2, aberrant GluA1 homomers form, and aberrant GluA2 and GluA3 homomers can also form in the absence of other subunits. Importantly, the fact that the various subunit deletions complement each other arithmetically suggests that compensation probably does not affect our central findings—the proportional contribution of each subunit to synaptic and extrasynaptic receptors.

Most Synaptic and Extrasynaptic AMPARs Are GluA1A2 Heteromers

Previous biochemical studies have suggested that most AMPARs in the hippocampus are heteromers composed of either GluA1A2 or GluA2A3 subunits (Wenthold et al., 1996). However, these investigations likely studied mixed populations of AMPARs, including ones from synaptic, extrasynaptic, and intracellular pools, in different cell types. Thus the subunit composition of synaptic and extrasynaptic AMPARs in CA1 pyramidal neurons remains uncertain. A comparison of the results from genetic experiments using germline KOs also failed to provide crucial insight into subunit composition of synaptic AMPARs. For instance, the deletion of GluA1 has been reported to have no effect (Zamanillo et al., 1999) or modest effects (Andrasfalvy et al., 2003) on synaptic transmission, suggesting that synaptic receptors are composed mainly of GluA2A3 heteromeric receptors. On the other hand, deletion of GluA3 has no effect on synaptic transmission (Meng et al., 2003), suggesting that synaptic receptors are not GluA2A3 heteromers. We thus employed conditional KO mice for GluA1, -A2, and -A3 to study the subunit composition of synaptic and extrasynaptic AMPARs.

As has been reported before, the I/Vs of AMPAR EPSCs are near linear (Adesnik and Nicoll, 2007; Bredt and Nicoll, 2003; Hestrin et al., 1990; Malinow and Malenka, 2002; Shepherd and Huganir, 2007), suggesting that virtually all synaptic AMPARs contain the GluA2 subunit. However, biochemical studies (Sans et al., 2003; Wenthold et al., 1996) indicate that GluA1 homomers are present in the hippocampus, raising the possibility that GluA1 homomers may exist at extrasynaptic locations. In agreement with earlier reports (Andrasfalvy and Magee, 2004; Rozov et al., 1998; Spruston et al., 1995), we find that the I/Vs of AMPAR-mediated currents from OOPs of CA1 pyramidal neurons are near linear, suggesting little contribution of GluA2-lacking receptors to extrasynaptic AMPARs. As an additional test for the presence of GluA2-lacking receptors, we employed PhTx-433 that potently blocks GluA2-lacking receptors (Washburn and Dingledine, 1996). Few studies have addressed the polyamine sensitivity (and thus the GluA2 content) of extrasynaptic receptors in these neurons. Concentrations of PhTx-433 that we established completely blocked extrasynaptic AMPAR currents from GluA2 KO mice had no effect on WT responses, ruling out any significant contribution of GluA2-lacking receptors in 2- to 3-week-old CA1 pyramidal neurons. Thus, virtually all functional AMPARs on the surface of CA1 pyramidal cells contain GluA2, and the small population of GluA1 homomers detected by biochemical methods is likely located in other hippocampal cells or the intracellular pool of AMPARs in CA1 pyramidal neurons.

It should be pointed out that the RI in WT neurons was typically less than 1 (approximately 0.9), both for the synaptic and the extrasynaptic currents. A comparison of the I/Vs for WT and GluA2 KO neurons obtained from voltage ramps (Figure 1) shows a fundamental difference in the shape of the curves. For the GluA2 KO, the strongest rectification occurs between 0 and +20 mV, whereas for the WT the current slowly becomes slightly less steep at more-positive membrane potentials. Although not commented on, this lack of linearity has been observed in previous studies in which spermine was added to the pipette solution, both for extrasynaptic (Andrasfalvy and Magee, 2004; Andrasfalvy et al., 2003; Rozov et al., 1998) and synaptic responses (Adesnik and Nicoll, 2007). This effect on WT AMPAR currents from hippocampal pyramidal neurons is due to the presence of 100 μM spermine in the pipette (Koh et al., 1995), a finding that we have confirmed (our unpublished data). Furthermore, it is important to keep in mind that the shape of the I/V curves can be modulated by several variables, independent of GluA2 content, most prominently by TARP association (Cho et al., 2007; Soto et al., 2007; Turetsky et al., 2005). Given the effects of intracellular spermine concentration and TARP association on the shape of the I/V curve, we conclude that the slight deviation from geometric linearity does not reflect the presence of GluA2-lacking receptors and that PhTx-433 provides a definitive test for probing the GluA2 content of AMPARs.

Deletion of GluA1 results in an ~95% loss of somatic extrasynaptic receptors (Figures 6A and 6B), in agreement with previous results (Andrasfalvy et al., 2003; Zamanillo et al., 1999), and an ~80% loss of synaptic currents (Figure 6C), which is significantly greater than that reported for the germline KO (Andrasfalvy et al., 2003; Zamanillo et al., 1999). Presumably this difference is attributable to compensation in the germline KO and emphasizes the significant advantage of using postnatal and focal genetic manipulations. One of the studies (Andrasfalvy et al., 2003) reported that the effect of deleting GluA1 is more prominent at distal synapses, raising the possibility of some heterogeneity in the AMPARs, depending on their locations. The finding that the I/Vs of the remaining synaptic and extrasynaptic

AMPAR-mediated responses in cells lacking GluA1 are linear strongly suggests that the remaining receptors are GluA2A3 heteromers. Consistent with this conclusion is the finding that deletion of GluA3 results in an ~16% reduction in synaptic currents and little change in the extrasynaptic currents (Figure 6). Thus, based on the results of deleting GluA1 and GluA3 individually, it would appear that ~16% of synaptic receptors and virtually none of the extrasynaptic receptors are GluA2A3 heteromers.

Our conclusion that GluA2A3 receptors are a small fraction of the total number of synaptic AMPARs in CA1 pyramidal neurons is also supported by a number of different experimental approaches. First, single-cell PCR studies show nearly equal amounts of GluA1 and GluA2 but less than one-tenth of these amounts for GluA3 in hippocampal pyramidal neurons (Geiger et al., 1995; Tsuzuki et al., 2001). Second, immunogold EM studies report similar labeling for GluA1 and GluA2 (Jensen et al., 2003; Sans et al., 2003). Third, proteomic studies of postsynaptic density (PSD) proteins from cortex and hippocampus indicate that GluA1 and GluA2 are present in approximately equal amounts, whereas GluA3 is presence at roughly one-fifth of these amounts (Cheng et al., 2006). Thus, understanding the trafficking of the GluA1A2 heteromer as a functional entity will be important for understanding how the receptor traffics in its native environment. On the other hand, given the modest contribution of GluA2A3 heteromers to synaptic transmission and the lack of obvious behavior defects in the GluA3 KO (Meng et al., 2003), the function of this population of receptors is unclear.

Implications for AMPAR Trafficking

Since the discovery of silent synapses, AMPAR trafficking has been a leading molecular mechanism underlying synaptic plasticity (Bredt and Nicoll, 2003; Kerchner and Nicoll, 2008; Malinow and Malenka, 2002; Shepherd and Huganir, 2007). Based on a variety of experiments in which GluA subunits were overexpressed in culture preparations, a leading model for constitutive and activity-dependent AMPAR trafficking has been advanced (Hayashi et al., 2000; Malinow and Malenka, 2002; Passafaro et al., 2001; Shi et al., 2001). In this model, basal synaptic transmission is primarily mediated by GluA2A3 heteromers, which undergo constitutive cycling into and out of synapses. LTP is achieved by the selective synaptic delivery of GluA1A2 heteromers, which otherwise are excluded from synapses. The synaptic trafficking of GluA1A2 heteromers is determined by the GluA1 subunit, and once arriving at synapses, GluA1A2 heteromers are gradually replaced by the cycling GluA2A3 heteromers. In contrast, a number of studies have suggested that the GluA2 subunit dictates the removal of AMPARs from the synapse during LTD (Bredt and Nicoll, 2003; Collingridge et al., 2004; Malinow and Malenka, 2002; Shepherd and Huganir, 2007). However, previous genetic evidence does not support a necessary role of GluA1 and GluA2 in LTP and LTD, respectively. Although LTP induced by tetanic stimulation is absent from CA1 in the adult GluA1 KO mouse, it can still be evoked in CA1 neurons from juvenile mice on which most physiological experiments on Schaffer collateral LTP have actually been performed (Jensen et al., 2003; Zamanillo et al., 1999), and it can also be induced in the adult with theta burst stimulation (Hoffman et al., 2002). In addition, a knockin strategy has actually revealed that GluA1 is critical for AMPAR endocytosis and LTD expression in hippocampus (Lee et al., 2003). Furthermore, in mice lacking both GluA2 and -A3, LTD is normal (Meng et al., 2003). Perhaps some of this discrepancy could be explained by the suggestion that recombinant receptors formed in hippocampal slice cultures are largely aberrantly expressed homomers (Shi et al., 2001) and may function differently from heteromers (Oh and Derkach, 2005), and/or plasticity experiments in germline KO mice may suffer from undesired compensatory effects, as discussed above.

Our results indicate that all subunit combinations, including heteromers as well as homomers, can traffic to synapses at CA1 pyramidal neurons, indicating that each subunit has an inherent capacity for synaptic targeting. This in turn suggests the existence of a basic AMPAR trafficking mechanism independent of receptor subunit composition. We have previously found that stargazin-like TARPs bind to all AMPAR subunits and, via their binding to PSD-95 and related MAGUKs, target receptors to synapses (Chen et al., 2000; Nicoll et al., 2006; Osten and Stern-Bach, 2006; Schnell et al., 2002; Ziff, 2007). Such a mechanism could provide the basis for our present findings.

Although AMPARs with different subunit combinations appear at the synapse, certain subunits were found to be more important in synaptic targeting than others. In the absence of GluA2, AMPARs were abundant at extrasynaptic sites, but targeting to the synapse was considerably impaired, indicating a specific role for GluA2 in AMPAR synaptic targeting. Previous evidence showed that interference with the GluA2 interaction with NSF led to rundown of synaptic transmission (Luscher et al., 1999; Luthi et al., 1999; Song et al., 1998), suggesting that the GluA2-NSF interaction may be involved in edited GluA2 homomer trafficking to synapses. Interestingly, based on the analysis of mEPSCs, we conclude that there is heterogeneity among synapses; some synapses are incapable of receiving GluA2-lacking receptors, and others accept a full complement. These synaptic deficits in GluA2-deleted cells are similar to those obtained in the GluA2 germline KO mouse (Panicker et al., 2008). The basis for this heterogeneity is unknown, although a similar heterogeneity has been reported for the involvement of MAGUKs in AMPAR synaptic trafficking (Beique et al., 2006; Elias et al., 2006). In addition, the observation that, in the absence of extrasynaptic receptors, a substantial number of GluA2 homomeric receptors target to the synapse further emphasizes a specific role of GluA2 in synaptic targeting. Finally, the fact that GluA1 homomers, formed in neurons lacking both GluA2 and -A3, can maintain normal extrasynaptic AMPAR currents suggests that GluA1 alone is sufficient for trafficking AMPARs to the neuronal surface. Previous evidence has shown that the carboxyl termini of AMPAR subunits are differentially involved in receptor trafficking (Bredt and Nicoll, 2003; Malinow and Malenka, 2002; Shepherd and Huganir, 2007), which may provide a mechanism for these differences on AMPAR targeting following various AMPAR subunit deletions. It is possible that the TARP-dependent regulation of AMPAR trafficking interacts with subunit-specific targeting mechanisms to generate the dynamic trafficking behavior of AMPARs at synapses (Ziff, 2007), which underlies synaptic plasticity in hippocampus. It will also be interesting to determine in the future to what degree TARPs can differentially traffic AMPARs with different subunit compositions.

Homomeric Receptors and Their Significance

In analogy to potassium channels (Tu and Deutsch, 1999), there is now general agreement that AMPARs are assembled as dimers of dimers (Ayalon et al., 2005; Ayalon and Stern-Bach, 2001; Mansour et al., 2001; Tichelaar et al., 2004). Although rules governing dimerization of dimers are still poorly understood, it has been proposed that a relatively high abundance of GluA2 in the endoplasmic reticulum (ER) facilitates the incorporation of GluA2 into final tetramers (Greger et al., 2002, 2007). As a result, in WT neurons that express GluA2, virtually all synaptic and extrasynaptic AMPARs contain GluA2. However, this assembly process is finely tuned, because GluA1 homomers immediately appear and traffic to synapses following a small drop in GluA2 expression (Figure 4A). Results from cells lacking GluA1 and -A3 or GluA1 and -A2 indicate that GluA2 and -A3 also form homotetrameric receptors. Interestingly, the GluA2 homomers that we recorded contain edited subunits, because the I/Vs of the remaining currents are linear. However, trafficking of edited GluA2 homomers appears to be inefficient, as only about 10% synaptic transmission remains in cells lacking both GluA1 and -A3 (Figure 5A2). Such inefficient trafficking of edited GluA2 homomers has been reported before (Greger et al., 2002). While AMPARs of all possible subunit combinations can assemble in neurons, it seems likely that homomeric receptor formation only occurs when heteromeric assembly is not an option and would thus play little role under normal conditions in CA1 pyramidal neurons.

Engineering an AMPAR Null Synapse

An important observation in this study is the loss of all functional surface AMPARs in cells lacking GluA1, -A2, and -A3. This demonstrates that we have successfully accounted for all AMPARs on CA1 pyramidal cells. In addition, it confirms, using genetic techniques, an observation previously made pharmacologically with the AMPAR selective antagonist GYKI 53655 that fast excitatory synaptic transmission on CA1 pyramidal neurons is mediated entirely by the release of glutamate acting on AMPARs, with no contribution from kainate receptors or other receptors (Bureau et al., 1999; Castillo et al., 1997). Although there is evidence that GluA4 can contribute to synaptic transmission in the neonatal hippocampus (Zhu et al., 2000), it appears to play no role at 2 weeks of age and onward, nor is it upregulated in the absence of other subunits in our experimental condition. One of the most important findings of this study is our ability to genetically create an AMPAR null synapse at hippocampal pyramidal neurons, which appears to be entirely normal in all other respects that we have examined. Thus, the normal NMDAR EPSCs indicate that synaptic targeting and retention of these receptors are independent of AMPARs and that there is no change in the number of synapses or probability in transmitter release. In accord with these physiological findings, we were unable to find structural abnormalities (i.e., dendritic length and branching or spine density) in cells devoid of AMPARs.

Based on previous studies, the preservation of synaptic structure and function in the absence of AMPARs is surprising. Spontaneous quantal activation of AMPARs is reported to be necessary for maintaining dendritic spines (Mateos et al., 2007; McKinney et al., 1999). In addition, the AMPAR GluA2 N-terminal domain is proposed to be critical for the formation and/or maintenance of dendritic spines (Passafaro et al., 2003; Saglietti et al., 2007). Finally, Aβ-induced synaptic depression is proposed to involve the removal of AMPARs, which in turn causes the loss of spines and synaptic NMDARs (Hsieh et al., 2006; Kopec et al., 2007; Venkitaramani et al., 2007). It is unclear what accounts for the discrepancies, although different experimental preparations (cultured neurons versus acute hippocampal slices in our studies) and different approaches (RNAi-mediated knockdown versus single-cell KO in vivo, and global manipulations versus cell-autonomous manipulations) may explain the differences. On the other hand, the natural existence of silent synapses in the brain (Isaac et al., 1995; Kerchner and Nicoll, 2008; Liao et al., 1995)—that is, synapses lacking AMPARs but containing NMDARs—suggests that the AMPAR is not an integral component required for formation and maintenance of spines. Furthermore, the preservation of normal synaptic anatomy and function in the absence of AMPARs is reminiscent of the stargazer phenotype, in which the mossy fiber synapses onto cerebellar granule cells lack AMPARs, but are otherwise anatomically and functionally normal (Chen et al., 2000; Hashimoto et al., 1999). This null phenotype proved invaluable in defining the role of stargazin, the mutated protein in the stargazer mouse, and also in the discovery that stargazin belongs to a family of auxiliary AMPAR subunits (Nicoll et al., 2006). Given the apparent lack of detectable change in anatomy or function of hippocampal synapses, such a null synapse provides the unique platform for a molecular replacement strategy, in which the molecular mechanism(s) of AMPAR trafficking in vivo can be investigated.

EXPERIMENTAL PROCEDURES

Electrophysiology

Acute transverse 300 μm hippocampal slices were prepared as described in the Supplemental Data. Cultured slices were prepared as previously described (Schnell et al., 2002). All paired recordings involved simultaneous whole-cell recordings from one GFP-positive neuron and a neighboring GFP-negative neuron, as described in the Supplemental Data.

Anatomy and Imaging

CA1 pyramidal cells were filled with Alexa Fluor 568 dyes through the patch pipette for about 5–10 min. After filling, slices were fixed, mounted, and scanned with confocal microscopy as described in the Supplemental Data.

SUPPLEMENTAL DATA

The Supplemental Data include supplemental text and one figure and can be found with this article online at http://www.neuron.org/supplemental/S0896-6273(09)00255-4.

ACKNOWLEDGMENTS

We thank Hillel Adesnik for help on neonatal injections, Aaron Milstein for Igor software, and Ye Bing for neuronal morphology. We thank the Nicoll lab members for discussions, as well as Pierre Apostolides for help in slice cultures. We are grateful to G. Kerchner, A. Milstein, G. Elias, M. Howard, and T. Hnasko for critical comments on the manuscript. P.H.S. and R.S. are funded by the Max Planck Society and EUSynapse. W.L. is funded by a postdoctoral fellowship from the American Heart Association, A.C.J. is funded by a National Research Service Award (NRSA) postdoctoral fellowship from the National Institutes of Health (NIH), and R.A.N. is funded by grants from the National Institute of Mental Health (NIMH).

Accepted: February 14, 2009
Published: April 29, 2009

REFERENCES

Adesnik, H., and Nicoll, R.A. (2007). Conservation of glutamate receptor 2-containing AMPA receptors during long-term potentiation. J. Neurosci. *27*, 4598–4602.

Adesnik, H., Nicoll, R.A., and England, P.M. (2005). Photoinactivation of native AMPA receptors reveals their real-time trafficking. Neuron *48*, 977–985.

Andrasfalvy, B.K., and Magee, J.C. (2004). Changes in AMPA receptor currents following LTP induction on rat CA1 pyramidal neurones. J. Physiol. *559*, 543–554.

Andrasfalvy, B.K., Smith, M.A., Borchardt, T., Sprengel, R., and Magee, J.C. (2003). Impaired regulation of synaptic strength in hippocampal neurons from GluR1-deficient mice. J. Physiol. *552*, 35–45.

Ayalon, G., and Stern-Bach, Y. (2001). Functional assembly of AMPA and kainate receptors is mediated by several discrete protein-protein interactions. Neuron *31*, 103–113.

Ayalon, G., Segev, E., Elgavish, S., and Stern-Bach, Y. (2005). Two regions in the N-terminal domain of ionotropic glutamate receptor 3 form the subunit oligomerization interfaces that control subtype-specific receptor assembly. J. Biol. Chem. *280*, 15053–15060.

Barria, A., and Malinow, R. (2002). Subunit-specific NMDA receptor trafficking to synapses. Neuron *35*, 345–353.

Bats, C., Groc, L., and Choquet, D. (2007). The interaction between Stargazin and PSD-95 regulates AMPA receptor surface trafficking. Neuron *53*, 719–734.

Baude, A., Nuzzer, Z., Molnar, E., McIlhinney, R.A.J., and Somogyi, P. (1995). High-resolution immunogold localization of AMPA type glutamate receptor subunits at synaptic and non-snaptic sites in rat hipppocampus. Neuroscience *69*, 1031–1055.

Beique, J.C., Lin, D.T., Kang, M.G., Aizawa, H., Takamiya, K., and Huganir, R.L. (2006). Synapse-specific regulation of AMPA receptor function by PSD-95. Proc. Natl. Acad. Sci. USA *103*, 19535–19540.

Bellone, C., and Nicoll, R.A. (2007). Rapid bidirectional switching of synaptic NMDA receptors. Neuron *55*, 779–785.

Bredt, D.S., and Nicoll, R.A. (2003). AMPA receptor trafficking at excitatory synapses. Neuron *40*, 361–379.

Bureau, I., Bischoff, S., Heinemann, S.F., and Mulle, C. (1999). Kainate receptor-mediated responses in the CA1 field of wild-type and GluR6-deficient mice. J. Neurosci. *19*, 653–663.

Burnashev, N., Monyer, H., Seeburg, P.H., and Sakmann, B. (1992). Divalent ion permeability of AMPA receptor channels is dominated by the edited form of a single subunit. Neuron *8*, 189–198.

Carmignoto, G., and Vicini, S. (1992). Activity-dependent decrease in NMDA receptor responses during development of the visual cortex. Science *258*, 1007–1011.

Castillo, P.E., Malenka, R.C., and Nicoll, R.A. (1997). Kainate receptors mediate a slow postsynaptic current in hippocampal CA3 neurons. Nature *388*, 182–186.

Chen, L., Chetkovich, D.M., Petralia, R.S., Sweeney, N.T., Kawasaki, Y., Wenthold, R.J., Bredt, D.S., and Nicoll, R.A. (2000). Stargazin regulates synaptic targeting of AMPA receptors by two distinct mechanisms. Nature *408*, 936–943.

Cheng, D., Hoogenraad, C.C., Rush, J., Ramm, E., Schlager, M.A., Duong, D.M., Xu, P., Wijayawardana, S.R., Hanfelt, J., Nakagawa, T., et al. (2006). Relative and absolute quantification of postsynaptic density proteome isolated from rat forebrain and cerebellum. Mol. Cell. Proteomics *5*, 1158–1170.

Cho, C.H., St-Gelais, F., Zhang, W., Tomita, S., and Howe, J.R. (2007). Two families of TARP isoforms that have distinct effects on the kinetic properties of AMPA receptors and synaptic currents. Neuron *55*, 890–904.

Collingridge, G.L., Isaac, J.T., and Wang, Y.T. (2004). Receptor trafficking and synaptic plasticity. Nat. Rev. Neurosci. *5*, 952–962.

Collingridge, G.L., Olsen, R.W., Peters, J., and Spedding, M. (2008). A nomenclature for ligand-gated ion channels. Neuropharmacology *56*, 2–5.

Cull-Candy, S., Kelly, L., and Farrant, M. (2006). Regulation of Ca2+-permeable AMPA receptors:synaptic plasticity and beyond. Curr. Opin. Neurobiol. *16*, 277–280.

Dingledine, R., Borges, K., Bowie, D., and Traynelis, S.F. (1999). The glutamate receptor ion channels. Pharmacol. Rev. *51*, 7–61.

Elias, G.M., Funke, L., Stein, V., Grant, S.G., Bredt, D.S., and Nicoll, R.A. (2006). Synapse-specific and developmentally regulated targeting of AMPA receptors by a family of MAGUK scaffolding proteins. Neuron *52*, 307–320.

Engblom, D., Bilbao, A., Sanchis-Segura, C., Dahan, L., Perreau-Lenz, S., Balland, B., Parkitna, J.R., Lujan, R., Halbout, B., Mameli, M., et al. (2008). Glutamate receptors on dopamine neurons control the persistence of cocaine seeking. Neuron *59*, 497–508.

Geiger, J.R., Melcher, T., Koh, D.S., Sakmann, B., Seeburg, P.H., Jonas, P., and Monyer, H. (1995). Relative abundance of subunit mRNAs determines gating and Ca2+ permeability of AMPA receptors in principal neurons and interneurons in rat CNS. Neuron *15*, 193–204.

Greger, I.H., Khatri, L., and Ziff, E.B. (2002). RNA editing at arg607 controls AMPA receptor exit from the endoplasmic reticulum. Neuron *34*, 759–772.

Greger, I.H., Ziff, E.B., and Penn, A.C. (2007). Molecular determinants of AMPA receptor subunit assembly. Trends Neurosci. *30*, 407–416.

Hashimoto, K., Fukaya, M., Qiao, X., Sakimura, K., Watanabe, M., and Kano, M. (1999). Impairment of AMPA receptor function in cerebellar granule cells of ataxic mutant mouse stargazer. J. Neurosci. *19*, 6027–6036.

Hayashi, Y., Shi, S.H., Esteban, J.A., Piccini, A., Poncer, J.C., and Malinow, R. (2000). Driving AMPA receptors into synapses by LTP and CaMKII: requirement for GluR1 and PDZ domain interaction. Science *287*, 2262–2267.

Hestrin, S., Nicoll, R.A., Perkel, D.J., and Sah, P. (1990). Analysis of excitatory synaptic action in pyramidal cells using whole- cell recording from rat hippocampal slices. J. Physiol. *422*, 203–225.

Hoffman, D.A., Sprengel, R., and Sakmann, B. (2002). Molecular dissection of hippocampal theta-burst pairing potentiation. Proc. Natl. Acad. Sci. USA *99*, 7740–7745.

Hollmann, M., and Heinemann, S. (1994). Cloned glutamate receptors. Annu. Rev. Neurosci. *17*, 31–108.

Hsieh, H., Boehm, J., Sato, C., Iwatsubo, T., Tomita, T., Sisodia, S., and Malinow, R. (2006). AMPAR removal underlies Abeta-induced synaptic depression and dendritic spine loss. Neuron *52*, 831–843.

Isaac, J.T., Nicoll, R.A., and Malenka, R.C. (1995). Evidence for silent synapses: implications for the expression of LTP. Neuron *15*, 427–434.

Isaac, J.T., Ashby, M., and McBain, C.J. (2007). The role of the GluR2 subunit in AMPA receptor function and synaptic plasticity. Neuron *54*, 859–871.

Jensen, V., Kaiser, K.M., Borchardt, T., Adelmann, G., Rozov, A., Burnashev, N., Brix, C., Frotscher, M., Andersen, P., Hvalby, O., et al. (2003). A juvenile form of postsynaptic hippocampal long-term potentiation in mice deficient for the AMPA receptor subunit GluR-A. J. Physiol. *553*, 843–856.

Jia, Z., Agopyan, N., Miu, P., Xiong, Z., Henderson, J., Gerlai, R., Taverna, F.A., Velumian, A., MacDonald, J., Carlen, P., et al. (1996). Enhanced LTP in mice deficient in the AMPA receptor GluR2. Neuron *17*, 945–956.

Jonas, P. (2000). The time course of signaling at central glutamatergic synapses. News Physiol. Sci. *15*, 83–89.

Kaspar, B.K., Vissel, B., Bengoechea, T., Crone, S., Randolph-Moore, L., Muller, R., Brandon, E.P., Schaffer, D., Verma, I.M., Lee, K.F., et al. (2002). Adeno-associated virus effectively mediates conditional gene modification in the brain. Proc. Natl. Acad. Sci. USA *99*, 2320–2325.

Kerchner, G.A., and Nicoll, R.A. (2008). Silent synapses and the emergence of a postsynaptic mechanism for LTP. Nat. Rev. Neurosci. *9*, 813–825.

Koh, D.S., Burnashev, N., and Jonas, P. (1995). Block of native Ca(2+)-permeable AMPA receptors in rat brain by intracellular polyamines generates double rectification. J. Physiol. *486*, 305–312.

Kopec, C.D., Real, E., Kessels, H.W., and Malinow, R. (2007). GluR1 links structural and functional plasticity at excitatory synapses. J. Neurosci. *27*, 13706–13718.

Lee, H.K., Takamiya, K., Han, J.S., Man, H., Kim, C.H., Rumbaugh, G., Yu, S., Ding, L., He, C., Petralia, R.S., et al. (2003). Phosphorylation of the AMPA receptor GluR1 subunit is required for synaptic plasticity and retention of spatial memory. Cell *112*, 631–643.

Liao, D., Hessler, N.A., and Malinow, R. (1995). Activation of postsynaptically silent synapses during pairing-induced LTP in CA1 region of hippocampal slice. Nature *375*, 400–404.

Luscher, C., Xia, H., Beattie, E.C., Carroll, R.C., von Zastrow, M., Malenka, R.C., and Nicoll, R.A. (1999). Role of AMPA receptor cycling in synaptic transmission and plasticity. Neuron *24*, 649–658.

Luthi, A., Chittajallu, R., Duprat, F., Palmer, M.J., Benke, T.A., Kidd, F.L., Henley, J.M., Isaac, J.T., and Collingridge, G.L. (1999). Hippocampal LTD expression involves a pool of AMPARs regulated by the NSF-GluR2 interaction. Neuron *24*, 389–399.

Malinow, R., and Malenka, R.C. (2002). AMPA receptor trafficking and synaptic plasticity. Annu. Rev. Neurosci. *25*, 103–126.

Mansour, M., Nagarajan, N., Nehring, R.B., Clements, J.D., and Rosenmund, C. (2001). Heteromeric AMPA receptors assemble with a preferred subunit stoichiometry and spatial arrangement. Neuron *32*, 841–853.

Mateos, J.M., Luthi, A., Savic, N., Stierli, B., Streit, P., Gahwiler, B.H., and McKinney, R.A. (2007). Synaptic modifications at the CA3–CA1 synapse after chronic AMPA receptor blockade in rat hippocampal slices. J. Physiol. *581*, 129–138.

Mayer, M.L., and Armstrong, N. (2004). Structure and function of glutamate receptor ion channels. Annu. Rev. Physiol. *66*, 161–181.

McKinney, R.A., Capogna, M., Durr, R., Gahwiler, B.H., and Thompson, S.M. (1999). Miniature synaptic events maintain dendritic spines via AMPA receptor activation. Nat. Neurosci. *2*, 44–49.

Megias, M., Emri, Z., Freund, T.F., and Gulyas, A.I. (2001). Total number and distribution of inhibitory and excitatory synapses on hippocampal CA1 pyramidal cells. Neuroscience *102*, 527–540.

Meng, Y., Zhang, Y., and Jia, Z. (2003). Synaptic transmission and plasticity in the absence of AMPA glutamate receptor GluR2 and GluR3. Neuron *39*, 163–176.

Nicoll, R.A., Tomita, S., and Bredt, D.S. (2006). Auxiliary subunits assist AMPA-type glutamate receptors. Science *311*, 1253–1256.

Oh, M.C., and Derkach, V.A. (2005). Dominant role of the GluR2 subunit in regulation of AMPA receptors by CaMKII. Nat. Neurosci. *8*, 853–854.

Osten, P., and Stern-Bach, Y. (2006). Learning from stargazin: the mouse, the phenotype and the unexpected. Curr. Opin. Neurobiol. *16*, 275–280.

Panicker, S., Brown, K., and Nicoll, R.A. (2008). Synaptic AMPA receptor subunit trafficking is independent of the C terminus in the GluR2-lacking mouse. Proc. Natl. Acad. Sci. USA *105*, 1032–1037.

Passafaro, M., Piech, V., and Sheng, M. (2001). Subunit-specific temporal and spatial patterns of AMPA receptor exocytosis in hippocampal neurons. Nat. Neurosci. *4*, 917–926.

Passafaro, M., Nakagawa, T., Sala, C., and Sheng, M. (2003). Induction of dendritic spines by an extracellular domain of AMPA receptor subunit GluR2. Nature *424*, 677–681.

Philpot, B.D., Sekhar, A.K., Shouval, H.Z., and Bear, M.F. (2001). Visual experience and deprivation bidirectionally modify the composition and function of NMDA receptors in visual cortex. Neuron *29*, 157–169.

Rozov, A., Zilberter, Y., Wollmuth, L.P., and Burnashev, N. (1998). Facilitation of currents through rat Ca2+-permeable AMPA receptor channels by activity-dependent relief from polyamine block. J. Physiol. *511*, 361–377.

Saglietti, L., Dequidt, C., Kamieniarz, K., Rousset, M.C., Valnegri, P., Thoumine, O., Beretta, F., Fagni, L., Choquet, D., Sala, C., et al. (2007). Extracellular interactions between GluR2 and N-cadherin in spine regulation. Neuron *54*, 461–477.

Sans, N., Vissel, B., Petralia, R.S., Wang, Y.X., Chang, K., Royle, G.A., Wang, C.Y., O'Gorman, S., Heinemann, S.F., and Wenthold, R.J. (2003). Aberrant formation of glutamate receptor complexes in hippocampal neurons of mice lacking the GluR2 AMPA receptor subunit. J. Neurosci. *23*, 9367–9373.

Schnell, E., Sizemore, M., Karimzadegan, S., Chen, L., Bredt, D.S., and Nicoll, R.A. (2002). Direct interactions between PSD-95 and stargazin control synaptic AMPA receptor number. Proc. Natl. Acad. Sci. USA *99*, 13902–13907.

Seeburg, P.H. (1993). The TINS/TiPS Lecture. The molecular biology of mammalian glutamate receptor channels. Trends Neurosci. *16*, 359–365.

Shepherd, J.D., and Huganir, R.L. (2007). The cell biology of synaptic plasticity: AMPA receptor trafficking. Annu. Rev. Cell Dev. Biol. *23*, 613–643.

Shi, S., Hayashi, Y., Esteban, J.A., and Malinow, R. (2001). Subunit-specific rules governing AMPA receptor trafficking to synapses in hippocampal pyramidal neurons. Cell *105*, 331–343.

Shimshek, D.R., Bus, T., Kim, J., Mihaljevic, A., Mack, V., Seeburg, P.H., Sprengel, R., and Schaefer, A.T. (2005). Enhanced odor discrimination and impaired olfactory memory by spatially controlled switch of AMPA receptors. PLoS Biol. *3*, e354. 10.1371/journal.pbio.0030354.

Sommer, B., Kohler, M., Sprengel, R., and Seeburg, P.H. (1991). RNA editing in brain controls a determinant of ion flow in glutamate-gated channels. Cell *67*, 11–19.

Song, I., Kamboj, S., Xia, J., Dong, H., Liao, D., and Huganir, R.L. (1998). Interaction of the N-ethylmaleimide-sensitive factor with AMPA receptors. Neuron *21*, 393–400.

Soto, D., Coombs, I.D., Kelly, L., Farrant, M., and Cull-Candy, S.G. (2007). Stargazin attenuates intracellular polyamine block of calcium-permeable AMPA receptors. Nat. Neurosci. *10*, 1260–1267.

Spruston, N., Jonas, P., and Sakmann, B. (1995). Dendritic glutamate receptor channels in rat hippocampal CA3 and CA1 pyramidal neurons. J. Physiol. *482*, 325–352.

Tichelaar, W., Safferling, M., Keinanen, K., Stark, H., and Madden, D.R. (2004). The three-dimensional structure of an ionotropic glutamate receptor reveals a dimer-of-dimers assembly. J. Mol. Biol. *344*, 435–442.

Tsuzuki, K., Lambolez, B., Rossier, J., and Ozawa, S. (2001). Absolute quantification of AMPA receptor subunit mRNAs in single hippocampal neurons. J. Neurochem. *77*, 1650–1659.

Tu, L., and Deutsch, C. (1999). Evidence for dimerization of dimers in K+ channel assembly. Biophys. J. *76*, 2004–2017.

Turetsky, D., Garringer, E., and Patneau, D.K. (2005). Stargazin modulates native AMPA receptor functional properties by two distinct mechanisms. J. Neurosci. *25*, 7438–7448.

Venkitaramani, D.V., Chin, J., Netzer, W.J., Gouras, G.K., Lesne, S., Malinow, R., and Lombroso, P.J. (2007). Beta-amyloid modulation of synaptic transmission and plasticity. J. Neurosci. *27*, 11832–11837.

Washburn, M.S., and Dingledine, R. (1996). Block of alpha-amino-3-hydroxy-5-methyl-4-isoxazolepropionic acid (AMPA) receptors by polyamines and polyamine toxins. J. Pharmacol. Exp. Ther. *278*, 669–678.

Wenthold, R.J., Petralia, R.S., Blahos, J., II, and Niedzielski, A.S. (1996). Evidence for multiple AMPA receptor complexes in hippocampal CA1/CA2 neurons. J. Neurosci. *16*, 1982–1989.

Zamanillo, D., Sprengel, R., Hvalby, O., Jensen, V., Burnashev, N., Rozov, A., Kaiser, K.M., Koster, H.J., Borchardt, T., Worley, P., et al. (1999). Importance of AMPA receptors for hippocampal synaptic plasticity but not for spatial learning. Science *284*, 1805–1811.

Zhu, J.J., Esteban, J.A., Hayashi, Y., and Malinow, R. (2000). Postnatal synaptic potentiation: delivery of GluR4-containing AMPA receptors by spontaneous activity. Nat. Neurosci. *3*, 1098–1106.

Ziff, E.B. (2007). TARPs and the AMPA receptor trafficking paradox. Neuron *53*, 627–633.